42. Yoshioka S, Aso Y, Kojima S. Temperature dependence of bimolecular reactions associated with molecular mobility in lyophilized formulations. Pharm Res 2000; 17:923–927.
43. Yoshioka S, Tajima S, Aso Y, et al. Inactivation and aggregation of β-galactosidase in lyophilized formulation described by the Kohlrausch-Williams-Watts stretched exponential function. Pharm Res 2003; 20:1655–1660.
44. Yoshioka S, Aso Y, Miyazaki T. Negligible contribution of molecular mobility to degradation rate of insulin lyophilized with poly(vinylpyrrolidone). J Pharm Sci 2006; 95:939–943.

International Journal of Pharmaceutics 427 (2012) 372–378

Contents lists available at SciVerse ScienceDirect

International Journal of Pharmaceutics

journal homepage: www.elsevier.com/locate/ijpharm

Hydration of surfactant-modified and PEGylated cationic cholesterol-based liposomes and corresponding lipoplexes by monitoring a fluorescent probe and the dielectric relaxation time

Yoshie Maitani[a,*], Ayako Nakamura[a], Takumi Tanaka[a], Yukio Aso[b]

[a] Institute of Medicinal Chemistry, Hoshi University, Ebara 2-4-41, Shinagawa-ku, Tokyo 142-8501, Japan
[b] National Institute of Health Science, 1-8-1 Kamiyoga, Tokyo 158-8501, Japan

ARTICLE INFO

Article history:
Received 30 September 2011
Received in revised form 30 January 2012
Accepted 9 February 2012
Available online 18 February 2012

Keywords:
Cationic liposome
Cellular association
Dielectric relaxation time
Hydration
Laurdan
Lipoplex
PEGylation

ABSTRACT

For the optimization of plasmid DNA (pDNA)-cationic lipid complexes and lipoplex delivery, proper indexes of the physicochemical properties of lipoplexes are required. In general, the characteristics of lipoplexes are defined by particle size and zeta-potential at various mixing ratios of cationic liposomes and pDNA. In this study, we characterized the hydration level of surfactant-modified and PEGylated cationic cholesterol-based (OH-Chol) liposomes and their lipoplexes by monitoring both the fluorescent probe laurdan and the dielectric relaxation time. Fluorescence measurement using laurdan detected hydration of the headgroup of lipids in surfactant-modified liposomes and PEGylated DOTAP-liposomes, but hardly any fluorescence was detected in PEGylated OH-Chol-liposomes because the PEG layers may extend and cover the fluorescent maker. On the other hand, the measurement of dielectric relaxation time of water molecules revealed total hydration, including hydration of the PEG layer and the headgroup of cationic lipids. Furthermore, we found an inverse correlation between hydration level and cellular uptake of PEGylated lipoplexes ($R = 0.946$). This finding indicated that the dielectric relaxation time of water molecules provides an important indicator of hydration of liposome and lipoplexes along with the fluorescence intensity of laurdan.

1. Introduction

Plasmid DNA (pDNA) is now widely employed in gene therapeutic applications. However, a major obstacle to the clinical application of pDNA is its inefficient cellular uptake. One promising clinical delivery strategy involves the use of pDNA-cationic liposome complexes, known as lipoplexes, in which negatively charged pDNA binds electrostatically to cationic lipids, such as OH-Chol and DOTAP, in liposomes. Such lipoplexes form when cationic liposomes, frequently containing a neutral co-lipid as a helper lipid, such as DOPE, at a 1:1 molar ratio, are mixed with pDNA (Yang and Huang, 1997). Furthermore, to enhance gene delivery, surface modification of the liposomes with surfactants and polymers has been reported. We and Inoh et al. (Inoh et al., 2001; Igarashi et al., 2006) have reported previously that biosurfactant mannosylerythritol lipid-A (MEL-A)-modified liposomes increased gene transfection efficiency in vitro. In in vivo gene delivery, poly(ethylene glycol) (PEG) polymer coating, PEGylation, has been reported frequently because colloidal particles, such as liposomes may be completely lost because of the capture of liposomes by macrophages in the liver and spleen (Blume and Cevc, 1990; Klibanov et al., 1990). PEGylation reduces the extent of uptake by macrophages and enhances the circulation time of liposomes in blood (Woodle et al., 1992; Allen et al., 1995). The underlying mechanism of the stabilization has been explained mainly through hydrated PEG chains on the surface.

In the optimization of lipoplex delivery, indexes of the physicochemical properties of lipoplexes are required. In general, the characteristics of lipoplexes are defined by particle size and zeta-potential at various mixing ratios of cationic liposome and pDNA. The hydration level of surface-modified and PEGylated liposomes has rarely been reported. A semi-quantitative approach for determining changes in the generalized polarization (GP) of laurdan was recently used successfully to characterize changes in hydration at lipid–water interfaces (Meidan et al., 2000). Measurement of dielectric relaxation time provides information on the structure of the hydration layer of colloids that interact with water

Abbreviations: OH-Chol, cholesteryl-3β-carboxyamindoethylene-*N*-hydroxyethylamine; DOPE, dioleoylphosphatidylethanolamine; DOTAP, dioleoyl-3-trimethylammonium propane; DSPE, distearoylphosphatidylethanolamine; DSPE-PEG2000, DSPE-polyethyleneglycol molecular weight 2000; MEL-A, mannosylerythritol lipid-A.

* Corresponding author. Tel.: +81 3 5498 5048; fax: +81 3 5498 5048.
E-mail address: yoshie@hoshi.ac.jp (Y. Maitani).

0378-5173/$ – see front matter © 2012 Elsevier B.V. All rights reserved.
doi:10.1016/j.ijpharm.2012.02.018

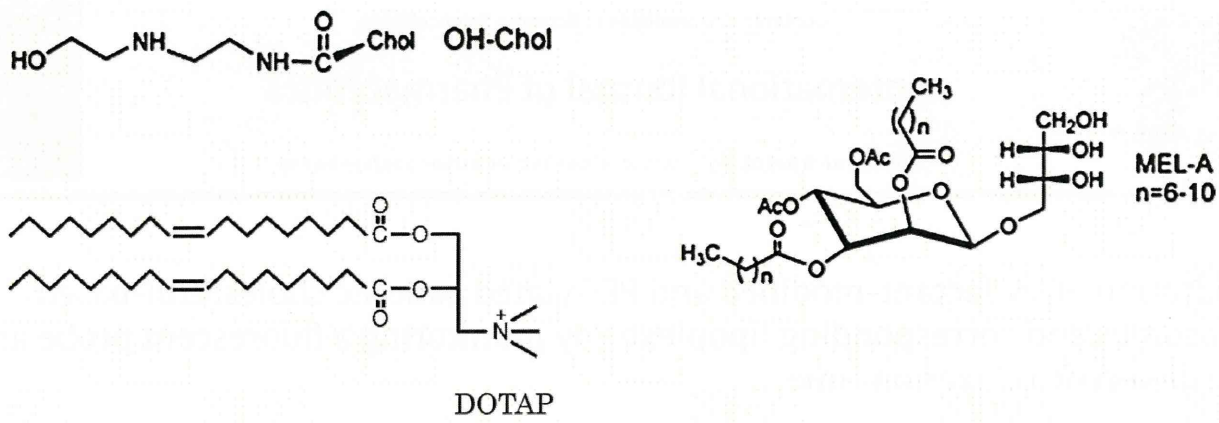

Fig. 1. Chemical structures of cholesteryl-3β-carboxyamindoethylene-*N*-hydroxyethylamine (OH-Chol), dioleoyl-3-tri-methylammonium propane (DOTAP) and mannosylerythritol lipid-A (MEL-A).

(Sato et al., 2007). In addition, the interactions of polar probe molecules with different environments present in such systems can be investigated. The process of dipolar relaxation may be related to the number of water molecules around the fluorescent moiety of laurdan. To the best of our knowledge, this is the first study to characterize the hydration of surfactant-modified and PEGylated cationic cholesterol-based liposomes and lipoplexes by measurement of dielectric relaxation time and to make a comparison with the GP value.

In this study, liposomes (~130 nm diameter) composed of either OH-Chol/DOPE/MEL-A (molar ratio 1:1:1) or OH-Chol/DOPE/Tween 80 (molar ratio 1:1:0.5) were employed as a model of surfactant-modified cationic cholesterol-based liposomes. PEGylated liposomes (~140 nm diameter) composed of OH-Chol/DOPE/DSPE/DSPE-PEG2000 (molar ratio 1:1:*x*:0.1−*x*) or DOTAP/Chol/DSPE/DSPE-PEG2000 (molar ratio 1:1:*x*:0.4−*x*) were employed as a model of PEGylated cationic cholesterol-based liposomes.

The present study aimed to examine the impact of surfactant-modification and PEGylation on the hydration of liposome and their lipoplexes by both monitoring lipid hydration level by the emission characteristics of the fluorescent probe laurdan included in the lipid bilayer and measurement of the dielectric relaxation time. Furthermore, the relationship between hydration of PEGylated lipoplexes, cellular association and transfection efficiency was investigated.

2. Materials and methods

2.1. Materials

OH-Chol was synthesized as reported previously (Fig. 1) (Takeuchi et al., 1996; Hattori et al., 2005). DOPE, Tween 80, DSPE and DSPE-PEG2000 (DSPE-PEG) were obtained from NOF Co., Ltd. (Tokyo, Japan), and MEL-A was purified as reported previously (Kitamoto et al., 1998) (Fig. 1). 6-Dodecanoyl-2-demethylaminonaphthalene (laurdan) was purchased from Lambda (Graz, Austria). DOTAP was purchased from Avanti Polar Lipids, Inc. (Alabaster, AL, USA) (Fig. 1). Plasmid DNA (pDNA), encoding the luciferase gene was constructed as described previously (Igarashi et al., 2006). A protein-free preparation of pDNA was purified following alkaline lysis using Maxiprep columns (Qiagen, Hilden, Germany). Fluorescein-labeled pDNA (FITC-DNA) was synthesized using pDNA and a fluorescein labeling kit (Mirus, Madison, WI, USA). Lipofectamine 2000 (Lipofectamine) was purchased from Invitrogen Corp. (Carlsbad, CA, USA).

2.2. Preparation of liposomes and lipoplexes

OH-Chol was formulated into liposomes with DOPE at a molar ratio of 1/1, and MEL-A or Tween 80 as a surfactant (OH-Chol/DOPE/surfactant = 1:1:1 or 1:1:0.5, respectively), which were prepared by a modified ethanol injection method (Hattori et al., 2005) with a cationic lipid concentration of 4.5 mM. The formulations were as reported previously (Ding et al., 2009a). Two kinds of PEGylated liposomes were formulated with OH-Chol or DOTAP as cationic lipids and designated OH-Chol-liposomes (OH-Chol/DOPE/DSPE/DSPE-PEG = 1:1:*x*:0.1−*x*) and DOTAP-liposomes (DOTAP/Chol/DSPE/DSPE-PEG = 1:1:*x*:0.4−*x*, molar ratio), respectively, prepared by a dry film method with a cationic lipid concentration of 4.5 mM. DSPE was used to compensate for changes in lipid membrane fluidity and electric charge by the addition of PEG-DSPE. The size of liposomes was adjusted by sonication with bath-typed sonicator. Here, unspecialized cationic liposomes indicate OH-Chol-liposomes.

To measure the hydration level of the liposomal surface, 0.2% (molar % to total lipids) laurdan was incorporated into the lipids. Lipoplexes at a charge ratio (+/−, amine in cationic lipids/pDNA phosphate ratio) of 3 or 5 were prepared by adding an aliquot of pDNA to each liposome mix and standing at room temperature for 5 min.

The size and zeta-potential of liposomes and lipoplexes were measured using an ELS-Z2 (Otsuka Electronics Co., Ltd., Osaka, Japan) in Milli Q water (water) (Elix® equipment, Millipore, MA, USA) or 1/10 phosphate-buffered saline (pH 7.4, 1/10 PBS).

2.3. Generalized polarization (GP) measurement

Twenty microliters of 0.2 mol% laurdan-labeled liposomes were diluted to 2 mL with PBS to a cationic lipid concentration of 0.045 mM. Lipoplexes were prepared by adding 40.8 μL liposomes to 59.2 μL pDNA (20 μg/mL of pDNA) and incubating for 5 min. After 20 μL of lipoplexes were diluted to 2 mL with PBS or water to a cationic lipid concentration of 0.0186 mM with 0.2 μg/mL of pDNA, laurdan fluorescence was measured by scanning emission wavelengths between 440 and 490 nm with an excitation wavelength of 340 nm (bandwidth 5 nm) at 25 °C in a Shimadzu RF-5300PC, as reported previously (Ding et al., 2009a). Cationic lipid concentrations of liposome (0.019–0.045 mM) increased GP values slightly with the increase in lipid concentration. Spectra were obtained at 0 min (not specially described) and at 30 min after dilution of the lipoplex mix with water or PBS. Laurdan is a membrane probe highly sensitive to environmental polarity, and it displays a large

red shift in emission in polar solvents with respect to nonpolar solvents (Parasassi et al., 1991). It is possible to follow the interfacial water changes in the cationic liposomes upon their complexation with pDNA by means of the spectral variations of laurdan (Parasassi et al., 1991) and by calculating the GP value as follows:

$$GP = \frac{(I_{440} - I_{490})}{(I_{440} + I_{490})} \quad (1)$$

wherein I_{440} and I_{490} are the emission intensities at wavelengths of 440 nm and 490 nm, respectively, with an excitation wavelength of 340 nm (Parasassi et al., 1991; Hirsch-Lerner and Barenholz, 1999). A higher GP value represents a lower hydration level (dehydration) on the liposomal surface. GP values were calculated from the absolute values of fluorescence intensity from one measurement, which was run in the same day with strictly controlled conditions. The repeated experiments showed different values, but with a similar trend.

The effect of pDNA on the GP value for various cationic liposomes is described as

$$\Delta GP = GP \text{ of lipoplex} - GP \text{ of liposome} \quad (2)$$

2.4. Dielectric relaxation time measurement

Dielectric relaxation time of water molecules was measured using a digitizing oscilloscope (model 54120B, Agilent Technologies) at 25 °C in water as reported previously (Yoshioka et al., 1995). At total lipid concentrations of 10–30 mg/mL, dielectric relaxation time did not change (data not shown); therefore, a total lipid concentration of 11.2 mg/mL, corresponding to 9 mM cationic lipid, was used.

2.5. Transfection protocol and luciferase activity measurement

The human lung adenocarcinoma A549 cell line was kindly provided by OncoTherapy Science. The cells were maintained in RPMI-1640 medium supplemented with 10% FBS and kanamycin (100 mg/mL) at 37 °C in a 5% CO_2 humidified incubator. Cells at a confluence level of 70% in a 22-mm culture dish were transfected with each lipoplex. For transfection, the prepared lipoplexes with 1 μg of pDNA were diluted in 500 μL of culture medium and then incubated with the cells for 24 h. For transfection with Lipofectamine as a control, 2.5 μL of Lipofectamine was used for 1 μg of pDNA to form a complex in Opti-MEM, in accordance with the manufacturer's protocol. Luciferase expression in A549 cells was measured as counts per second (cps)/μg protein using the luciferase assay system (Picagene, Tokyo Ink Mfg. Co., Ltd., Tokyo, Japan) and the cps value was normalized to the protein concentration, as determined using a bicinchoninic acid protein assay (Pierce, Rockford, IL, USA).

2.6. Flow cytometry

A549 cells were prepared by plating in a 35-mm culture dish 24 h prior to each experiment. Each liposome was mixed with 2 μg of FITC-DNA at a charge ratio (+/−) of 3:1, and then diluted in 1 mL of PBS. Cells were incubated with the lipoplexes at 37 °C for 2 h. After incubation, the cells were washed two times with PBS and detached with 0.05% trypsin and centrifuged at 1500 rpm for 3 min. The supernatant was discarded and the cell pellets were resuspended with PBS containing 0.1% BSA and 1 mM EDTA. The suspended cells were introduced directly into a FACSCalibur flow cytometer (Becton Dickinson, CA, USA). Data for 10,000 fluorescent events were obtained by recording forward scatter (FSC), side scatter (SSC), and green fluorescence. Mean intensity values of FITC inside cells were calculated to compare the uptake amount of lipoplexes.

2.7. Statistical analysis

The statistical significance of differences between mean values was determined using Welch's *t*-test. Multiple comparisons were evaluated by analysis of variance (ANOVA) with Tukey's multiple comparison test. *P*-values less than 0.05 were considered significant. All experiments were repeated at least two times.

3. Results and discussion

Previously we reported that lipoplexes of MEL-A-modified liposomes (OH-Chol/DOPE/MEL-A = 1:1:0.5) and Tween 80-modified liposomes showed higher gene transfection efficiency at a charge ratio of (+/−) 3 than at a charge ratio of 5 (Ding et al., 2009b). In addition, the GP value of MEL-A-modified liposomes (OH-Chol/DOPE/MEL-A = 1:1:1) was slightly higher compared with that of liposomes with a lower MEL-A ratio (OH-Chol/DOPE/MEL-A = 1:1:0.5) (Ding et al., 2009a). Therefore, in this study, we used MEL-A-modified liposomes with a 1:1:1 (OH-Chol/DOPE/MEL-A) composition. To examine the hydration levels of MEL-A-modified, Tween 80-modified and PEGylated liposomes, and their lipoplexes, at charge ratios of (+/−) 3 and 5, GP values and dielectric relaxation times were measured and compared.

3.1. Surfactant-modified liposomes and lipoplexes

3.1.1. Size and zeta-potential

The mean particle size of non-modified liposomes and MEL-A- and Tween 80-modified liposomes in water was approximately 130 nm, which was adjusted by sonication. An increase in the charge ratio (+/−) from 3 to 5 increased the zeta-potential of all lipoplexes. In lipoplexes at charge ratios of (+/−) 3 and 5, MEL-A-modified liposomes exhibited a slightly decreased zeta-potential compared with non-modified lipoplexes, but Tween 80 increased it in water (Fig. 2A). These trends were also observed in lipoplexes in 1/10 PBS, although the each zeta-potential was decreased (Fig. 2B). The change in zeta-potential of lipoplexes suggested that the cationic part of OH-Chol was affected by modification of MEL-A and Tween 80.

3.1.2. Hydration monitoring fluorescent probe

The GP value depends mainly on changes in hydration of the bilayer headgroup region either because of changes in the ratio between the less hydrated gel phase and the more hydrated liquid-crystalline phase and gel phase, or because of dependency on the pH in the range 4–10 and the type of polar headgroup (Lerner and Barenholz, 2007).

Fluorescence measurements were undertaken before and after addition of appropriate amounts of pDNA to laurdan-labeled liposomes at charge ratios of (+/−) 3 and 5. The results showed that the mean GP value for liposomes was 0.395 (at a cationic lipid concentration of 0.019 mM) (Fig. 3A). The corresponding values for MEL-A- or Tween 80-modified liposomes were 0.420 and 0.327, respectively (Fig. 3A). MEL-A dehydrated the liposomal surface, while Tween 80 hydrated it, corresponding well with a previous report (Ding et al., 2009a). Because Tween 80 possesses twenty oxyethylene residues in the hydrophilic region, and MEL-A possesses only three hydroxyl groups, the water molecules bound per Tween 80 would be much higher than those per MEL-A (Ding et al., 2009a). Interestingly liposomes and lipoplexes showed the same trend for changes in GP values after surfactant modification.

After pDNA addition, the ΔGP value for the three systems was investigated. Lipoplexes at a charge ratio of (+/−) 3 demonstrated positive ΔGP values, but at a charge ratio of (+/−) 5, lipoplexes showed small negative ΔGP values (Fig. 3B). Positive

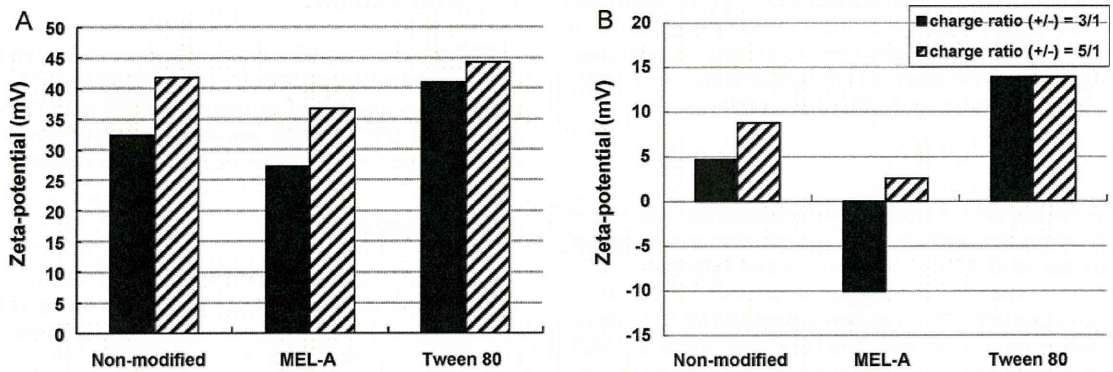

Fig. 2. Zeta-potential of surfactant-modified lipoplexes at charge ratios of (+/−) 3 and 5 in water (A) and 1/10 PBS (B). Each value represents the mean ($n=2$).

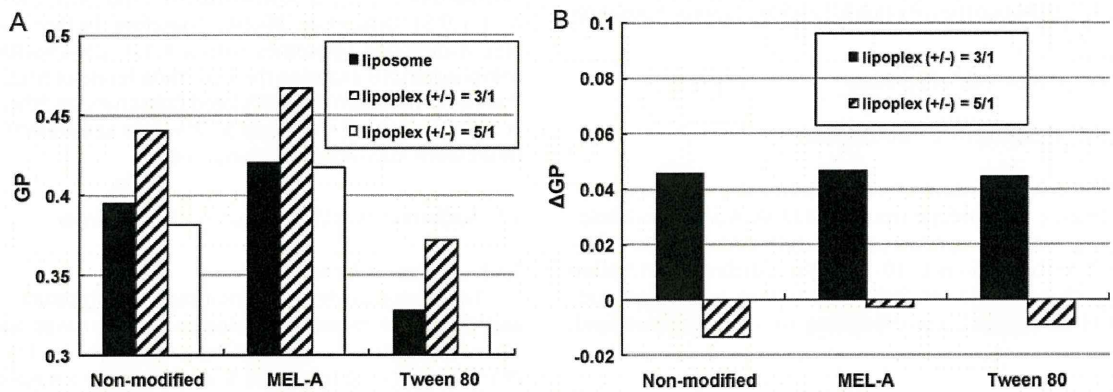

Fig. 3. The change of surface hydration of surfactant-modified liposomes and lipoplexes at charge ratios of (+/−) 3 and 5 as monitored by laurdan generalized polarization (GP) (A) and ΔGP (B) values in PBS. Each value represents the mean ($n=2$).

values of ΔGP indicate lower hydration levels than the corresponding liposome formulations (Hirsch-Lerner and Barenholz, 1999; Meidan et al., 2000), i.e. the interaction of cationic lipids with pDNA reduced hydration at the water–lipid interface (Luciani et al., 2007), Negative values of ΔGP indicate that the free headgroups of cationic lipids projected outside of the lipoplex and were hydrated, which indicates excess cationic liposomes. These findings support the increased zeta-potentials of MEL-A- and Tween 80-modified lipoplexes with the increase in charge ratio of (+/−) from 3 to 5. In other words, more positively charged MEL-A- or Tween 80-modified lipoplexes with a charge ratio of (+/−) 5 were more hydrated than those with a charge ratio of (+/−) 3. Hereafter we focus on lipoplexes with a charge ratio of (+/−) 3, where liposomes interact minimally with pDNA.

3.1.3. *Hydration monitoring dielectric relaxation time*

The result of dielectric relaxation time of water molecules in the liposome suspensions revealed that MEL-A-modified liposome exhibited significantly decreased dielectric relaxation times (10.32 ± 0.08 ps) compared with non-modified liposomes (10.87 ± 0.05 ps), and Tween 80-modified liposomes slightly increased it (11.1 ± 0.19 ps) (Fig. 4), indicating dehydration and hydration of liposomes, respectively, compared with non-modified liposomes. Lipoplexes at a charge ratio of (+/−) 3 showed similar trends for dielectric relaxation times compared with liposomes alone. The dielectric relaxation times between liposomes and lipoplexes cannot be compared directly, because hydration of the polar groups of pDNA, such as deoxyribose, is considered to contribute to the dielectric relaxation time of water molecules in lipoplex suspensions.

These findings for GP value and dielectric relaxation time of surfactant-modified liposomes and lipoplexes showed similar trends, indicating that the hydrated outer layer was associated with headgroups of OH-Chol, and pDNA interacts with this part. The change in GP values of liposomes and lipoplexes at a charge ratio of (+/−) 3 indicated that water was excluded from the lipid headgroup region when heterogeneous condensation of cationic lipids by pDNA took place.

As reported previously (Ding et al., 2009a), in terms of the cellular association of surfactant-modified liposomes, the relation of hydration level and zeta-potential to the cellular uptake was not

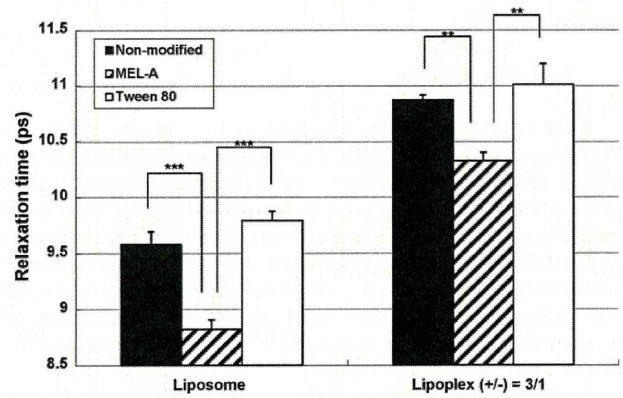

Fig. 4. Dielectric relaxation time of surfactant-modified liposomes and lipoplexes at a charge ratio of (+/−) 3 in water. Data represent mean ± S.D. ($n=3$). $^{*}P<0.05$, $^{**}P<0.01$, $^{***}P<0.001$.

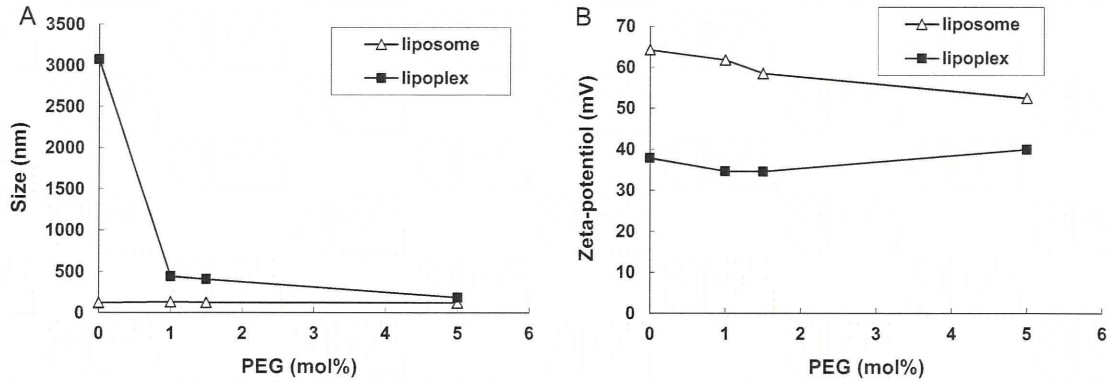

Fig. 5. Size (A) and zeta-potential (B) of PEGylated OH-Chol-liposomes at a charge ratio of (+/−) 3 in water. Each value represents the mean ($n = 2$).

clear for incubation with PBS for 2 h. The ions in PBS might interact with cationic charge on the relatively outer surface of the liposomes even covered with surfactants.

3.2. PEGylated liposomes and lipoplexes

3.2.1. Size and zeta-potential

The particle size and zeta-potentials of OH-Chol-liposomes were 121.9 nm and 64.3 mV, respectively in water (Fig. 5A and B). Without PEGylation, lipoplexes were likely to aggregate. Increasing the amount of PEGylation greatly decreased the lipoplex sizes (Fig. 5A) and did not largely change the zeta-potential of lipoplexes (Fig. 5B). Because the cationic lipid concentration was constant, this change in size is attributed to the packing effects of PEG chains into vesicle structures (Garbuzenko et al., 2005; Sato et al., 2007).

3.2.2. Hydration monitoring fluorescent probe

Next, to examine the effect of PEGylated cationic lipids on GP values, we measured GP values of PEGylated DOTAP-liposome (Fig. 6) and PEGylated OH-Chol-liposome (Fig. 7A). The particle size and zeta-potentials of DOTAP-Chol-liposomes from 0 to 20 mol% were 105.8 ± 1.3–142.7 ± 22.5 nm and 38.3 ± 1.3–45.7 ± 3.0 mV, respectively in water. The fluorescence of liposomes was recorded in PBS. A large decrease in GP values of liposomes at 5 mol% PEG, which are often used for PEGylation of liposomes. From these results, we focused on modification below 5 mol% PEG.

The fluorescence of OH-Chol-liposomes in PBS and lipoplexes was recorded GP and GP (0 min and 30 min) after dilution with PBS, respectively (Fig. 7A). Unlike with PEGylated DOTAP-liposomes, the values of PEGylated OH-Chol-liposome did not decrease largely

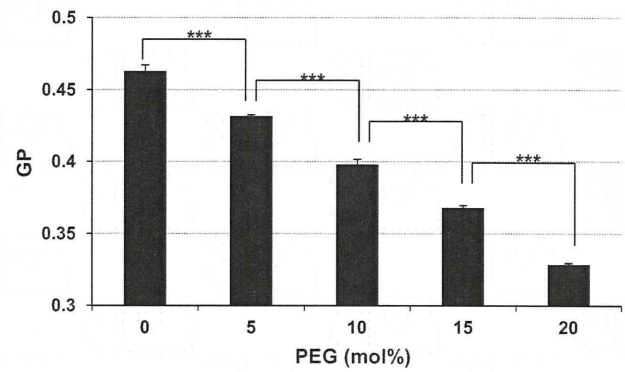

Fig. 6. The change of surface hydration of PEGylated DOTAP-liposome by PEGylation amount as monitored by laurdan generalized polarization (GP) in PBS at a charge ratio of (+/−) 3. Data represent mean ± S.D. ($n = 3$). ***$P < 0.001$.

at 5 mol% PEG. The GP values of OH-Chol-liposomes were higher than those of DOTAP-liposomes for all degrees of PEGylation. That is, PEGylated OH-Chol-liposomes were less hydrated, and PEGylated DOTAP-liposomes were more hydrated, corresponding with a previous report in which cholesterol induced the dehydration of lipid bilayers (Hirsch-Lerner and Barenholz, 1999; Meidan et al., 2000). Stepniewski et al. (2011) reported that PEG penetrates the lipid core of the membrane for the case of a liquid-crystalline membrane but is excluded from the tighter structure of the gel membrane. Because DOTAP-liposomes have more fluid membrane than OH-Chol-liposomes, the difference of changes in GP values by PEGylation may be as a result of the different structures of PEG

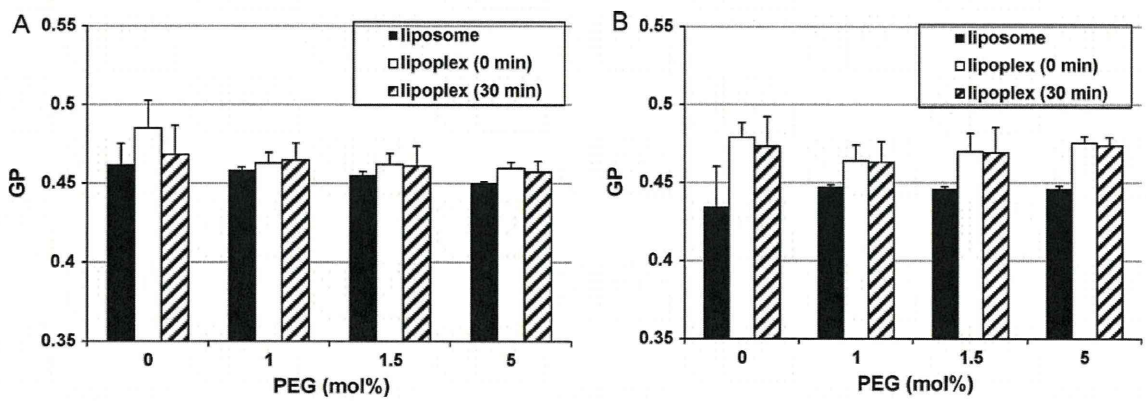

Fig. 7. The change of surface hydration of PEGylated OH-Chol-liposomes and lipoplexes at a charge ratio of (+/−) 3 as monitored by laurdan generalized polarization (GP) 0 min or 30 min after dilution with PBS (A) or water (B). Data represent mean ± S.D. ($n = 3$).

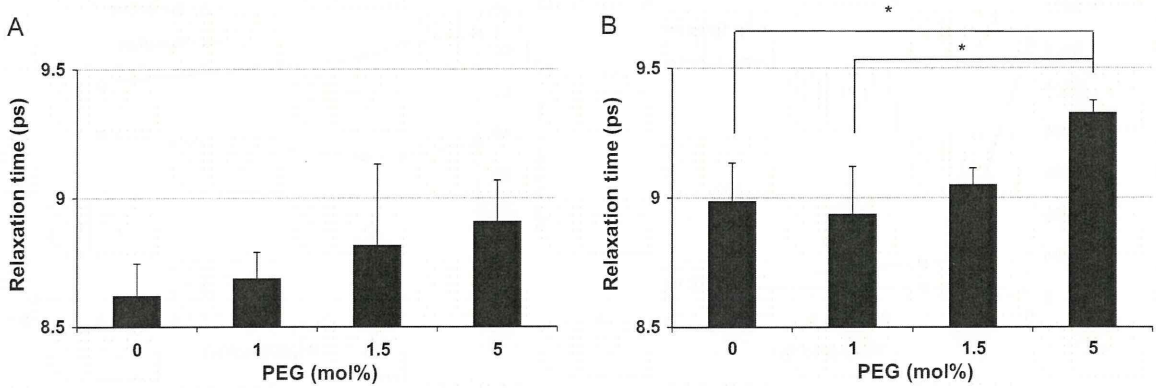

Fig. 8. Dielectric relaxation times of PEGylated OH-Chol-liposomes (A) and lipoplexes (B) at a charge ratio of (+/−) 3 in water. Data represent mean ± S.D. ($n = 3$). *$P < 0.05$.

on the liposomal membrane. PEG layers may cover and extend the fluorescence of laurdan at the headgroups of OH-Chol.

To examine the effect of the solvent on GP values, we also measured GP values of the same liposomes and lipoplexes in water. The GP values of PEGylated OH-Chol-liposomes and lipoplexes in water were similar to those in PBS (Fig. 7B). The GP (0 min and 30 min) values of lipoplexes at a charge ratio of (+/−) 3 hardly changed between PBS and water. The degrees of PEGylation were not reflected change of GP values.

3.2.3. *Hydration monitoring dielectric relaxation time*

Unlike the GP values, the dielectric relaxation times of PEGylated OH-Chol-liposome were longer with increasing amounts of PEG in water, indicating the hydrated PEG layer (Fig. 8A). In addition, the dielectric relaxation times of lipoplexes were significantly longer than those of non-PEGylated and 1 mol% PEGylated lipoplexes (Fig. 8B). These findings indicated that PEGylated liposomes and PEGylated lipoplexes were hydrated with increasing amounts of PEG.

In the present study, we measured dielectric relaxation time in a frequency range between 0.1 GHz and 20 GHz. A dielectric loss peak at approximately 10 GHz was observed for all the suspensions of surface-modified cationic liposomes and lipoplexes studied. The loss peak is considered to be because of the dielectric relaxation of bulk water and the relaxation of water hydrated to PEG and the headgroups of cationic lipid. For PEG and DSPE-PEG solutions, the relaxation time of hydrated water has been reported to be 5–6 times longer than that of bulk water (Sato et al., 2007). In the present study, the dielectric loss peak was not separated into each relaxation process because of the limitations of the measuring frequency of the instrument used (<20 GHz). Therefore, the relaxation time measured in the present study reflected both relaxation processes, and the longer relaxation time indicates a higher contribution of hydrated water of PEG with longer relaxation time than that of bulk water.

The influence of the surface-modification of cationic liposomes by surfactants and PEG-lipid on the hydration level of liposomes and the corresponding lipoplexes were examined by measurement of GP values of a fluorescent marker and of dielectric relaxation. In surfactant-modified liposomes, GP values and dielectric relaxation times demonstrated that liposomes modified with MEL-A and the corresponding lipoplexes were more dehydrated, but liposomes with Tween 80 were more hydrated compared with unmodified liposomes. In PEGylated liposomes, changes in GP values of liposome and lipoplexes were hardly observed at a charge ratio of (+/−) 3. Dielectric relaxation times in water demonstrated that more highly PEGylated liposomes and lipoplexes were more hydrated.

3.2.4. *Cellular association and transfection efficiency of PEGylated lipoplexes*

Finally to clarify the relationship between PEGylation and transfection levels, we examined the cellular association of lipoplexes using FITC-DNA in A549 cells incubated 2 h by flow cytometry. In Fig. 9A, with the presence of PEG-lipid in the lipoplexes, a significant decrease of cellular uptake was in each step from 159.9 ± 7.6 with non-PEGylated lipoplexes to 36.0 ± 0.6 with 5 mol% PEGylated lipoplexes. In accordance with this, the luciferase activity was decreasing roughly 150-fold from 75,444 cps/μg protein with non-PEGylation to 494 cps/μg protein with 5 mol% PEGylated lipoplexes (Fig. 9B).

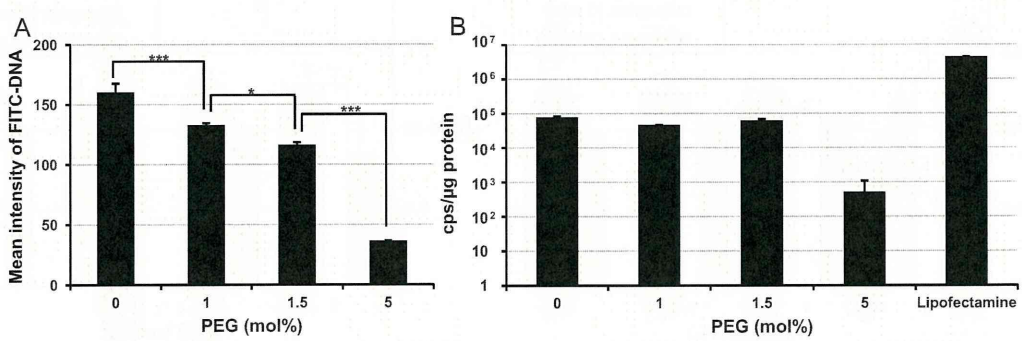

Fig. 9. Cellular association of FITC-DNA (A) and transfection efficiency (B) of PEGylated OH-Chol-liposomes at a charge ratio of (+/−) 3. Lipoplexes were incubated with A549 cells for 2 h in PBS measured by flow cytometry (A) and for 24 h in culture medium for gene transfections (B). Each result represents the mean ± S.D. ($n = 3$). ***$P < 0.001$ and *$P < 0.05$.

We found an inverse correlation between the amount of PEGylation in the lipoplexes and uptake in A549 cells. PEGylation significantly decreased the association of the lipoplexes at 2 h from the FITC intensities, corresponding with the result of DOTAP/cholesterol lipoplexes (Gjetting et al., 2010). The decreased cellular association of lipoplexes by PEGylation was probably caused by the steric barrier of PEG layers where the zeta-potential was not greatly changed by PEGylation between 34.57 and 39.98 mV (Fig. 5B). It was suggested that PEG layers may be projected out of the solid liposomes. In other words, the hydration level of PEG-lipid on liposomes by measurement of dielectric relaxation may reflect the projection level of PEG layers out of liposomes. Transfection efficiencies were not consistent with the result of cellular uptake except for 5 mol% PEGylation. Other factors might affect transfection efficiency more than cellular uptake. Until now, it has been speculated that there is a negative relationship between hydration ratio by PEGylation and cellular uptake of lipoplexes. This is the first study to measure hydration ratio of PEGylated lipoplexes and demonstrate that there is a correlation between hydration level and cellular uptake of PEGylated lipoplexes ($R = 0.946$). This indicates that PEGylation of liposomes may be attributed to hydration more than the cationic headgroups, which were monitored by dielectric relaxation times. Thus, the hydration of lipids is the proper index to evaluate the quality of PEGylated lipoplexes.

4. Conclusions

Fluorescence measurements with laurdan detected the hydration of headgroups of lipids in surfactant-modified OH-Chol-liposomes, but could not monitor the hydration in PEGylated OH-Chol-liposomes because PEG layers may cover and extend the fluorescence of laurdan in the headgroups of cationic lipids. On the other hand, the measurement of dielectric relaxation time detected the hydration of both surfactant-modified OH-Chol-liposomes and PEGylated OH-Chol-liposomes because the dielectric relaxation time of water revealed total hydration including hydration of the PEG layer and the headgroups of cationic lipids. This is the first report that dielectric relaxation time is a useful parameter for analysis of the hydration of liposomes and lipoplexes. These findings will help to select and provide optimal lipid formulations and surface modifications of liposomes, as well as optimal charge ratios of cationic liposomes and pDNA with fewer in vitro experiments.

Acknowledgements

This project was supported in part by the Open Research Center Project and by a grant for Research on Regulatory Science of Pharmaceuticals and Medical Devices from the Ministry of Health, Labor and Welfare.

References

Allen, T.M., Hansen, C.B., Lopes de Menezes, D.E., 1995. Pharmacokinetics of long circulating liposomes. Adv. Drug Deliv. Rev. 16, 267–284.

Blume, G., Cevc, G., 1990. One of the first publications demonstrating the prolonged circulation time of PEG-modified liposomes. Biochim. Biophys. Acta 1029, 91–97.

Ding, W., Hattori, Y., Qi, X., Kitamoto, D., Maitani, Y., 2009a. Surface properties of lipoplexes modified with mannosylerythritol lipid-A and Tween 80 and their cellular association. Chem. Pharm. Bull. 57, 138–143.

Ding, W., Izumisawa, T., Hattori, Y., Qi, X., Kitamoto, D., Maitani, Y., 2009b. Non-ionic surfactant modified cationic liposomes mediated gene transfection in vitro and in the mouse lung. Biol. Pharm. Bull. 32, 311–315.

Garbuzenko, O., Barenholz, Y., Priev, A., 2005. Effect of grafted PEG on liposome size and on compressibility and packing of lipid bilayer. Chem. Phys. Lipids 135, 117–129.

Gjetting, T., Arildsen, N.S., Christensen, C.L., Poulsen, T.T., Roth, J.A., Handlos, V.N., Poulsen, H.S., 2010. *In vitro* and *in vivo* effects of polyethylene glycol(PEG)-modified lipid in DOTAP/cholesterol-mediated gene transfection. Int. J. Nanomed. 5, 371–383.

Hattori, Y., Kubo, H., Higashiyama, K., Maitani, Y., 2005. Folate-linked nanoparticles formed with DNA complexes in sodium chloride solution enhance transfection efficiency. J. Biomed. Nanotechnol. 1, 176–184.

Igarashi, S., Hattori, Y., Maitani, Y., 2006. Biosurfactant MEL-A enhances cellular association and gene transfection by cationic liposome. J. Controlled Release 112, 362–368.

Inoh, Y., Kitamoto, D., Hirashima, N., Nakanishi, M., 2001. Biosurfactants of MEL-A increase gene transfection mediated by cationic liposomes. Biochem. Biophys. Res. Commun. 289, 57–61.

Kitamoto, D., Yanagisawa, H., Haraya, K., Kitamoto, H.K., 1998. Contribution of a chain-shortening pathway to the biosynthesis of the fatty acids of mannosylerythritol lipid (biosurfactant) in the yeast *Candida antarctica*: effect of β-oxidation inhibitors on biosurfactant synthesis. Biotechnol. Lett. 20, 813–818.

Klibanov, A.L., Maruyama, K., Torchilin, V.P., Huang, L., 1990. Amphipathic polyethyleneglycols effectively prolong the circulation time of liposomes. FEBS Lett. 268, 235–237.

Luciani, P., Bombelli, C., Colone, M., Giansanti, L., Ryhänen, S.J., Säily, V.M., Mancini, G., Kinnunen, P.K., 2007. Influence of the spacer of cationic gemini amphiphiles on the hydration of lipoplexes. Biomacromolecules 8, 1999–2003.

Hirsch-Lerner, D., Barenholz, Y., 1999. Hydration of lipoplexes commonly used in gene delivery: follow-up by laurdan fluorescence changes and quantification by differential scanning calorimetry. Biochim. Biophys. Acta 1461, 47–57.

Meidan, V.M., Cohen, J.S., Amariglio, N., Hirsch-Lerner, D., Barenholz, Y., 2000. Interaction of oligonucleotides with cationic lipids: the relationship between electrostatics, hydration and state of aggregation. Biochim. Biophys. Acta 1464, 251–261.

Parasassi, T., De Stasio, G., Ravagnan, G., Rusch, R.M., Gratton, E., 1991. Quantitation of lipid phases in phospholipid vesicles by the generalized polarization of Laurdan fluorescence. Biophys. J. 60, 179–189.

Sato, T., Sakai, H., Sou, K., Buchner, R., Tsuchida, E., 2007. Poly(ethylene glycol)-conjugated phospholipids in aqueous micellar solutions: hydration, static structure, and interparticle interactions. J. Phys. Chem. B 111, 1393–1401.

Stepniewski, M., Pasenkiewicz-Gierula, M., Róg, T., Danne, R., Orlowski, A., Karttunen, M., Urtti, A., Yliperttula, M., Vuorimaa, E., Bunker, A., 2011. Study of PEGylated lipid layers as a model for PEGylated liposome surfaces: molecular dynamics simulation and Langmuir monolayer studies. Langmuir 27, 7788–7798.

Takeuchi, K., Ishihara, M., Kawaura, C., Noji, M., Furuno, T., Nakanishi, M., 1996. Effect of zeta potential of cationic liposomes containing cationic cholesterol derivatives on gene transfection. FEBS Lett. 397, 207–209.

Woodle, M.C., Matthay, K.K., Newman, M.S., Hidayat, J.E., Collins, L.R., Redemann, C., Martin, F.J., Papahadjopoulos, D., 1992. Versatility in lipid compositions showing prolonged circulation with sterically stabilized liposomes. Biochim. Biophys. Acta 113, 193–200.

Yang, J.P., Huang, L., 1997. Overcoming the inhibitory effect of serum on lipofection by increasing the charge ratio of cationic liposome to DNA. Gene Ther. 4, 950–960.

Yoshioka, S., Aso, Y., Otsuka, T., Kojima, S., 1995. Water mobility in poly(ethylene glycol)-, poly(vinylpyrrolidone)-, and gelatine-water systems, as indicated by dielectric relaxation time, spin-lattice relaxation time, and water activity. J. Pharm. Sci. 84, 1072–1077.

Pharm Res (2011) 28:3237–3247
DOI 10.1007/s11095-011-0512-8

RESEARCH PAPER

Effect of Sugars on the Molecular Motion of Freeze-Dried Protein Formulations Reflected by NMR Relaxation Times

Sumie Yoshioka • Kelly M. Forney • Yukio Aso • Michael J. Pikal

Received: 23 November 2010 / Accepted: 10 June 2011 / Published online: 25 June 2011

ABSTRACT

Purpose To relate NMR relaxation times to instability-related molecular motions of freeze-dried protein formulations and to examine the effect of sugars on these motions.

Methods Rotating-frame spin-lattice relaxation time ($T_{1\rho}$) was determined for both protein and sugar carbons in freeze-dried lysozyme-sugar (trehalose, sucrose and isomaltose) formulations using solid-state ^{13}C NMR.

Results The temperature dependence of $T_{1\rho}$ for the lysozyme carbonyl carbons in lysozyme with and without sugars was describable with a model that includes two different types of molecular motion with different correlation times (τ_c) for the carbon with each τ_c showing Arrhenius temperature dependence. Both relaxation modes have much smaller relaxation time constant (τ_c) and temperature coefficient (Ea) than structural relaxation and may be classified as β-relaxation and γ-relaxation. The τ_c and Ea for γ-relaxation were not affected by sugars, but those for β-relaxation were increased by sucrose, changed little by trehalose, and decreased by isomaltose, suggesting that the β-mobility of the lysozyme carbonyl carbons is decreased by sucrose and increased by isomaltose.

Conclusion $T_{1\rho}$ determined for the lysozyme carbonyl carbons can reflect the effect of sugars on molecular mobility in lysozyme. However, interpretation of relaxation time data is complex and may demand data over an extended temperature range.

S. Yoshioka (✉) • K. M. Forney • M. J. Pikal
School of Pharmacy, University of Connecticut
Storrs, Connecticut 06269–3092, USA
e-mail: sumie.yoshioka@uconn.edu

Y. Aso
National Institute of Health Sciences
Setagaya, Tokyo 158–8501, Japan

KEY WORDS freeze-dried protein · molecular dynamics · NMR · relaxation time · sucrose

INTRODUCTION

Many researchers have recognized that the instability of pharmaceutical formulations in the amorphous state is correlated with the molecular dynamics (1–9). Correlations between instability and structural relaxation (10–18) or molecular motions with shorter timescales (β-relaxation or fast dynamics) (19–24) have been demonstrated for various amorphous formulations. For stability prediction and stabilization of freeze-dried protein (and labile small molecule) formulations, it is important to identify the motion most relevant to the instability, which largely depends on the degradation mechanisms and formulation components.

Various techniques have been used to determine molecular motions in amorphous formulations for proteins and small molecules. Structural relaxation has been characterized by dynamic mechanical measurements (25–27), isothermal microcalorimetry (28), differential scanning calorimetry (29), dielectric relaxation spectroscopy (30–32) and thermally stimulated depolarization current spectroscopy (33). Some of these techniques have also been used to characterize molecular dynamics on timescales shorter than structural relaxation. Fast dynamics of amorphous formulations on timescales much shorter than structural relaxation have been studied by neutron scattering and NMR relaxation measurements. Neutron scattering can probe atomic motions on the timescale of nanoseconds or shorter in freeze-dried formulations (22,23,34). NMR can detect atomic motions on the timescale of MHz and kHz, which are reflected by spin-lattice relaxation times in the

laboratory and rotating frames (T_1 and $T_{1\rho}$), respectively (35–37).

Although one might intuitively expect that instability of formulations would correlate best with structural relaxation because of the similar timescales of degradation and structural relaxation, correlations are often better with fast dynamics (20,22–24). For example, it has been demonstrated that NMR relaxation times T_1 and $T_{1\rho}$ are coupled with the instability of freeze-dried protein formulations. The $T_{1\rho}$ of the carbonyl carbons of freeze-dried insulin was increased by the addition of trehalose, which increased the storage stability of insulin (20). Sucrose, which increased the $T_{1\rho}$ of the protein carbonyl carbons more intensely than trehalose and stachyose, stabilized freeze-dried β-galactosidase more effectively than the others (24). These findings qualitatively suggest couplings between NMR fast dynamics and instability of freeze-dried protein formulations, but the mechanism of coupling is still unclear.

The purpose of this study is to quantify the timescales of molecular motions that are potentially coupled with instability and to elucidate the effect of sugars on these molecular motions. Here, $T_{1\rho}$ was determined for both protein and sugar carbons in freeze-dried protein formulations as a function of temperature using solid-state ^{13}C NMR. $T_{1\rho}$ is a NMR relaxation time, which does not directly indicate molecular mobility. Thus, the correlation time (τ_c) of the carbon, which indicates the time required for the carbon to rotate one radian, was determined from the temperature dependence of the observed $T_{1\rho}$. Trehalose, sucrose and isomaltose were used as excipients, and the well-studied protein lysozyme was used. Trehalose and sucrose are known to stabilize many freeze-dried proteins (20,24). Isomaltose is also a dissacharide with a similar molecular structure to trehalose and sucrose and has a T_g value between those of trehalose and sucrose. The effect of sugars on the τ_c of the carbon is discussed in relation to the stabilizing effects of these sugars. Furthermore, the temperature coefficient (apparent activation energy, Ea) of molecular motions is determined from the temperature dependence of τ_c and compared with the values reported for Ea as determined by other relaxation techniques, such as dynamic mechanical measurements, isothermal microcalorimetry and dielectric relaxation spectroscopy.

MATERIALS AND METHODS

Preparation of Freeze-Dried Formulations

Sucrose (S-9378, Sigma Chemical Co., St. Louis, MO, USA), trehalose (Pfanstiehl, Waukegan, IL, USA), isomaltose (400480–2 Seikagaku baio bijinesu Co., Tokyo, Japan) and ^{13}C-methyl isomaltose were freeze-dried with or without lysozyme (Sigma Chemical Co., St. Louis, MO, USA). ^{13}C-methyl isomaltose was prepared by methylating isomaltose with ^{13}C-methyl iodide (99% ^{13}C, Cambridge Isotope Laboratories, Inc., Andover, MA) using dimsyl sodium as a proton removal reagent (38).

Protein solutions (50 mg/mL) were prepared after dialysis against water. Protein : sugar solutions were prepared in a one-to-one ratio by diluting the protein solution to 25 mg/mL. Samples were prepared in 5 ml tubing glass vials (1 mL fill volume) and freeze-dried in a FTS Durastop freeze-drier (FTS Kinetics, Stoneridge, NY). The shelf temperature during primary drying was set at −25°C and increased at 0.1°C/min to 40°C for secondary drying and held for 6 h. Chamber pressure throughout drying was set at 80mTorr, and in all cases product temperature was maintained below collapse temperature. Vials were sealed in the chamber under vacuum using Daikyo Florotec stoppers and stored at −20°C until use. The water content determined by the Karl Fisher method was less than 0.2%. The glass transition temperature (T_g) measured by differential scanning calorimetry (TA Instruments) was 73°C for sucrose, 114°C for trehalose, 101°C for isomaltose, 88°C for lysozyme-sucrose, 131°C for lysozyme-trehalose and 109°C for lysozyme-isomaltose.

Determination of $T_{1\rho}$ of Lysozyme Carbonyl and Sugar Carbons by ^{13}C Solid-State NMR

The freeze-dried sample was added to a 4 mm Zirconia MAS rotor with a Macor cap (Wilmad LabGlass, Vineland, NJ), firmly, with the packing tool in a glove bag purged with dry nitrogen (relative humidity < 2%).

The $T_{1\rho}$ of each lysozyme carbonyl carbon and sugar carbon was determined at nominal (set) temperatures ranging from −70°C to 150°C (actual sample temperature: −57.3°C to 130.7°C) using a ^{13}C CP/MAS NMR operating at a proton resonance frequency of 300 MHz (Bruker DMX 300). The software used was Xwinnmr 2.6. Spin-locking field was equivalent to 62.5 kHz (^1H 90° pulse length was 4.0 μs). The spinning speed was 10 kHz. The contact time was 1.0 ms, and the recycling delay was 5 s. The maximum length of the spin locking pulse was varied with the $T_{1\rho}$ value from 4 ms to 30 ms. Signals were obtained at five spin locking pulse lengths. Signal acquisition was performed for 4–5 h at each data point except for the measurements to examine changes in $T_{1\rho}$ during heating below the T_g. Temperature was calibrated using ^{207}Pb MAS spectra of solid lead nitrate, as previously reported (39).

The NMR spectrum obtained for freeze-dried lysozyme is shown in Fig. 1, and those for trehalose, sucrose,

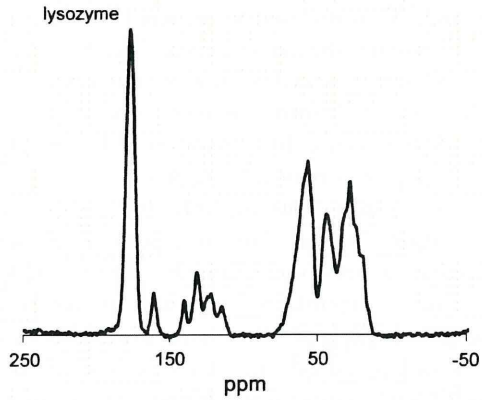

Fig. 1 NMR spectrum of freeze-dried lysozyme.

isomaltose, lysozyme-trehalose, lysozyme-sucrose and lysozyme-isomaltose are shown in Fig. 2. For the measurement of $T_{1\rho}$ for the lysozyme carbonyl carbons, the peak at approximately 175 ppm was used (observed $T_{1\rho}$ represents the average of that for all carbonyl carbons in all molecules of lysozyme). For the $T_{1\rho}$ measurement of trehalose carbon, the peak at 92 ppm belonging to the methine carbons (C-1 and C-1′) was used. The peak at 104 ppm belonging to the carbon (C-1) was used for the $T_{1\rho}$ measurement of sucrose carbon (40). For the $T_{1\rho}$ of isomaltose comprised of two anomers, the peak at 97 ppm, which mainly belongs to the methine carbon (C-1), was used. $T_{1\rho}$ was calculated by fitting the signal decay to a mono-exponential equation. τ_c was calculated from the $T_{1\rho}$ using the parameters estimated by fitting the $T_{1\rho}$ data to an equation describing the relationship between $T_{1\rho}$ and τ_c (described in the Discussion section) with the Origin 8.1 software (OriginLab Co., Northampton, MA).

Sub-T_g Heating of Freeze-Dried Lysozyme-Trehalose and Lysozyme-Sucrose

The effect of sub-T_g heating (i.e., annealing) on the $T_{1\rho}$ of the lysozyme carbonyl carbons was examined using freeze-dried lysozyme-trehalose and lysozyme-sucrose. Freeze-dried samples packed in the rotor were heated at 62°C for 8 h in the NMR probe with spinning at 10 kHz. Then, signal acquisition was started after temperature was lowered or raised to the target temperature.

In addition, the time dependence of changes in $T_{1\rho}$ during sub-T_g heating was examined by acquiring signals at −40°C, and then at 62°C, as a function of time. The duration required for a temperature change from −40°C to 62°C was 0.5 h. Signal acquisition at 62°C was started immediately after the temperature became constant and at intervals thereafter. Signal acquisition was carried out for 3 h at each time point.

RESULTS

Temperature Dependence for $T_{1\rho}$ of Lysozyme Carbonyl Carbons

The temperature dependence of the relaxation time is critical for the evaluation of the fundamental time constant, the molecular correlation time (τ_c). The time course of $T_{1\rho}$ relaxation for the carbonyl carbons of lysozyme was describable with the mono-exponential equation for all samples, both in the absence and the presence of sugars. Figure 3 shows the temperature dependence of the $T_{1\rho}$ calculated from the mono-exponential time course. The $T_{1\rho}$ of the carbonyl carbons in the absence of sugars and in the presence of trehalose and isomaltose exhibited a complex temperature dependence that shows two minima in the temperature ranges above 50°C and below 10°C, as well as a maximum at a temperature between 10°C and 90°C. For lysozyme freeze-dried with sucrose, $T_{1\rho}$ was not determined at temperatures above 90°C because of the possible complicating effects of a glass transition.

For the $T_{1\rho}$ minimum in the lower temperature range, the addition of sugars did not change the temperature at which the $T_{1\rho}$ minimum occurred. In contrast, for the $T_{1\rho}$ minimum in the higher temperature range, the minimum was impacted by the sugars with the effect of sugars on the temperature of $T_{1\rho}$ minimum varying with the sugar. Isomaltose significantly shifted the temperature of the $T_{1\rho}$ minimum to a lower temperature, whereas the effect of trehalose was not significant. Although the $T_{1\rho}$ minimum in the higher temperature range could not be directly observed for sucrose, sucrose shifted the temperature of the $T_{1\rho}$ maximum (which occurs between the two minima) to a higher temperature, suggesting that the $T_{1\rho}$ minimum is sifted to a higher temperature. Note also that the temperature of the $T_{1\rho}$ maximum was shifted to a lower temperature by isomaltose, whereas the effect of trehalose was not significant.

The value of $T_{1\rho}$ at the $T_{1\rho}$ minimum was increased by trehalose and isomaltose for both $T_{1\rho}$ minima in the lower and higher temperature ranges. Sucrose also increased the value of $T_{1\rho}$ at the $T_{1\rho}$ minimum in the lower temperature range. Trehalose exhibited the greatest effect on the $T_{1\rho}$ value at the minimum.

Effect of Sub-T_g Heating on $T_{1\rho}$ of Lysozyme Carbonyl Carbons

Annealing of freeze-dried formulations at temperatures below and near the T_g is well known to increase the α-relaxation time of the formulation (41). Thus, the change in $T_{1\rho}$ with time upon heating at a temperature below T_g was determined for the lysozyme carbonyl carbons in freeze-

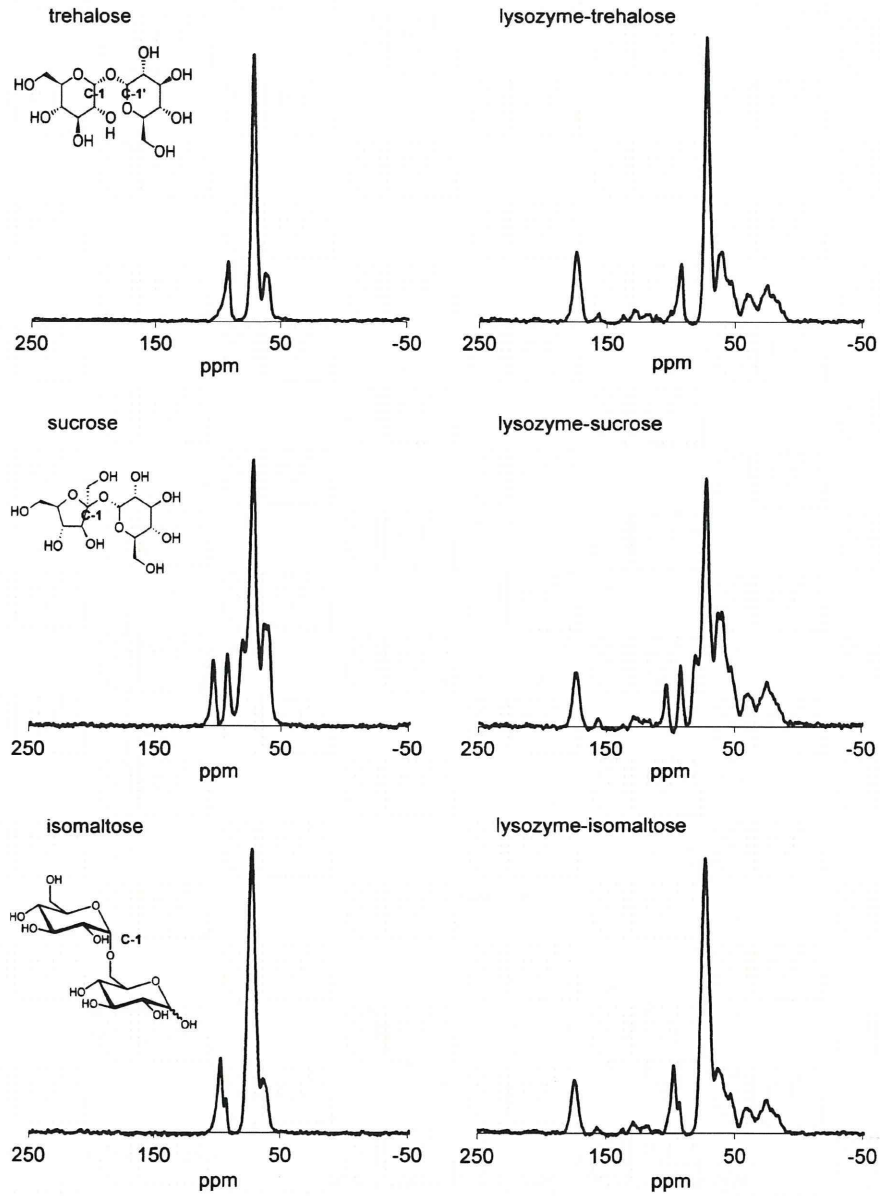

Fig. 2 NMR spectra of freeze-dried sugars and freeze-dried lysozyme with sugars.

dried lysozyme-trehalose and lysozyme-sucrose. Figure 4 shows the time dependence of changes in the $T_{1\rho}$ of the lysozyme carbonyl carbons associated with a temperature change from −40°C to 62°C. Similar changes were observed for both freeze-dried lysozyme-trehalose (Fig. 4a) and lysozyme-sucrose (Fig. 4b). Immediately after temperature was raised from −40°C to 62°C, $T_{1\rho}$ increased to a value similar to that determined at 62.3°C without the heating-cooling sequence, as shown in Fig. 3. Then, at a time shortly (≈ 3 hr) after the temperature rise, $T_{1\rho}$ sharply decreased. Thereafter, $T_{1\rho}$ gradually decreased further to an apparent equilibrium value.

Figure 5 compares the temperature dependence of $T_{1\rho}$ before and after heating at 62°C for 8 h. For both freeze-dried lysozyme-trehalose and lysozyme-sucrose, the values of $T_{1\rho}$ at temperatures above 0°C were greatly decreased by the heating treatment, whereas only small changes were observed at lower temperatures. The V-shaped temperature dependence of $T_{1\rho}$ observed for the sucrose system in the lower temperature range before heating was widened and the minimum moved toward higher temperature. For the trehalose system, the $T_{1\rho}$ minimum in the lower temperature range became obscure. We also found that the minimum in the high temperature range observed before heating was eliminated. These changes in $T_{1\rho}$ caused by sub-T_g heating indicate changes in the mobility of the carbon, the details of which will be described in the Discussion section.

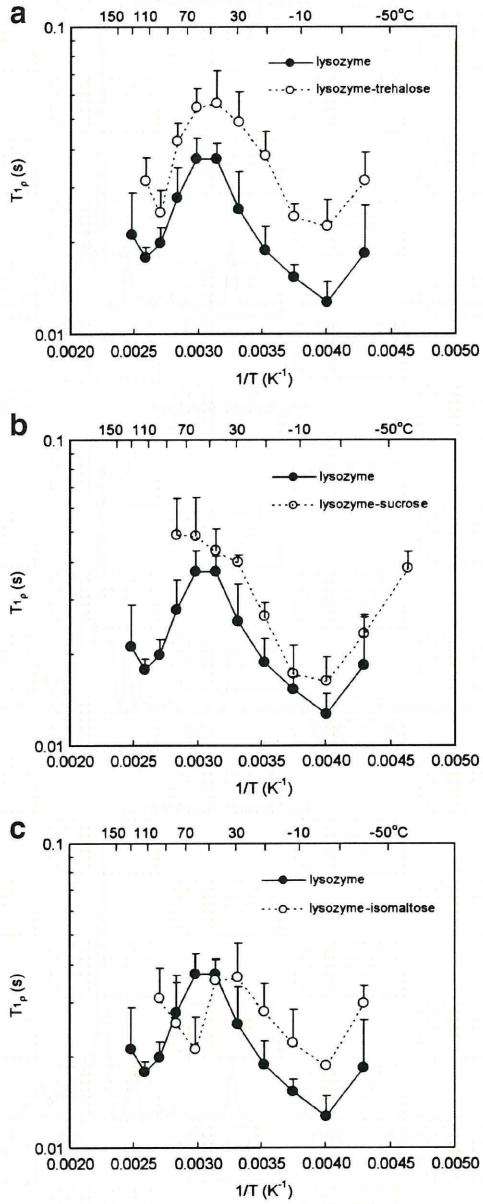

Fig. 3 Temperature dependence of $T_{1\rho}$ for lysozyme carbonyl carbons in freeze-dried lysozyme (**a**, **b**, **c**), lysozyme-trehalose (**a**), lysozyme-sucrose (**b**) and lysozyme-isomaltose (**c**) The error bars represent standard deviation ($n=3$).

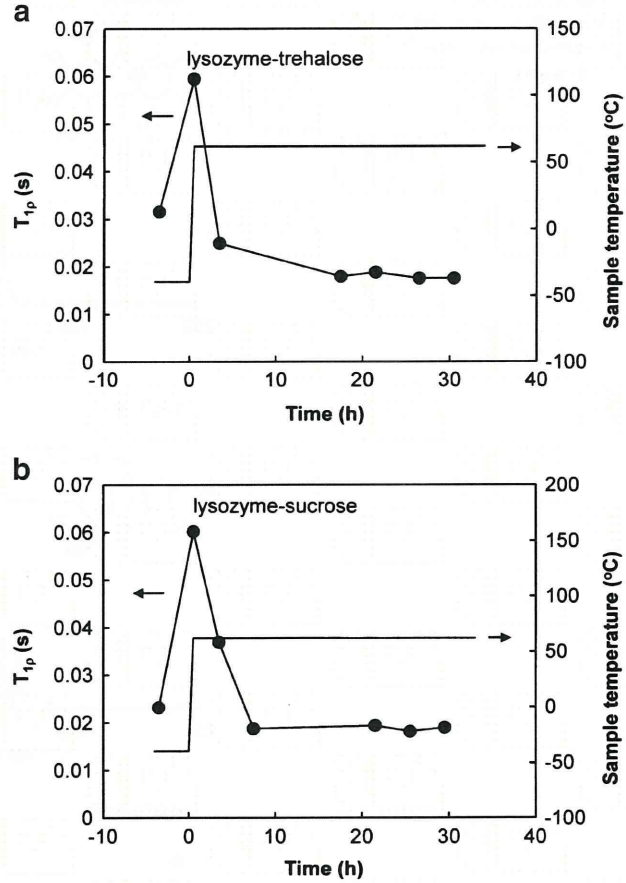

Fig. 4 Time dependence of changes in $T_{1\rho}$ of lysozyme carbonyl carbons in freeze-dried lysozyme-trehalose and lysozyme-sucrose. Temperature was increased from −40°C to 62°C at a time point of −0.5 h. The temperature reached 62°C at a time point of zero. Signal acquisition at 62°C was started at a time point of zero and at intervals thereafter. Signal acquisition was carried out for 3 h at each time point.

Temperature Dependence of $T_{1\rho}$ for Sugar carbon

The carbons of trehalose, sucrose and isomaltose (C-1 in Fig. 2) showed a peak separated from the peaks of the other methine carbons. Temperature dependence for the $T_{1\rho}$ of these carbons in the presence and absence of lysozyme is shown in Fig. 6 for the trehalose and sucrose carbons and in Fig. 7 for isomaltose. The addition of lysozyme did not bring about significant changes in the temperature dependence for the sugar carbons. The decrease in $T_{1\rho}$ observed in the high temperature range for the sucrose carbon was shifted to higher temperature by the addition of lysozyme most likely because of higher T_g of the lysozyme-sucrose system compared to the sucrose system.

Figure 7 also shows temperature dependence for the $T_{1\rho}$ of the methyl carbon introduced to the hydroxyl group of isomaltose. The methyl carbon exhibited a temperature dependence qualitatively similar to that of the methine carbon.

DISCUSSION

Mobility of Lysozyme Freeze-Dried with Sugars

The relationship between the correlation time τ_c and $T_{1\rho}$ of a given carbon can be described by Eq. 1, when

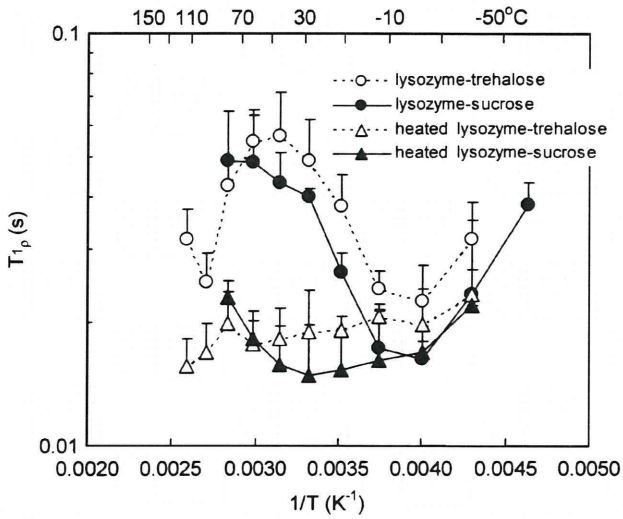

Fig. 5 Effect of heating on $T_{1\rho}$ of lysozyme carbonyl carbons in freeze-dried lysozyme-trehalose and lysozyme-sucrose. Heating was carried out at 62°C for 8 h. The error bars represent standard deviation ($n=3$).

the carbon has a single type of motion that shows a single τ_c.

$$\frac{1}{T_{1\rho}} = \frac{A\tau_c}{1+4\omega_1^2\tau_c^2} \tag{1}$$

where ω_1 is the strength of spin-locking and A is a constant determined by the gyromagnetic ratio of carbon, the number of protons involved in proton-carbon dipole interaction, which causes spin-lattice relaxation, and the distance between the carbon and the proton involved in the interaction. Because $T_{1\rho}$ becomes a minimum when $\tau_c = 1/2\omega_1$, the value of A can be determined from the

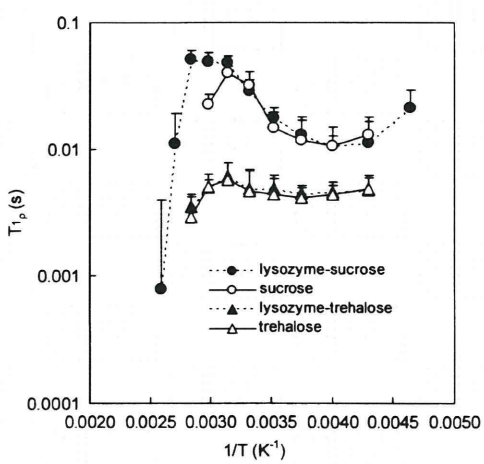

Fig. 6 Temperature dependence for $T_{1\rho}$ of carbons C-1 of trehalose and sucrose with and without lysozyme. The error bars represent standard deviation ($n=3$).

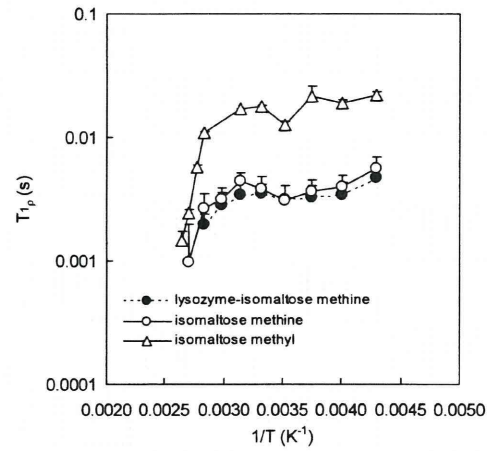

Fig. 7 Temperature dependence for $T_{1\rho}$ of carbon C-1 of isomaltose with and without lysozyme and temperature dependence for $T_{1\rho}$ of the methyl carbon of methylated isomaltose. The error bars represent standard deviation ($n=3$).

$T_{1\rho}$ value observed at the minimum ($T_{1\rho}$(min)) according to Eq. 2.

$$A = \frac{4\omega_1}{T_{1\rho}(\min)} \tag{2}$$

When the carbon has multiple types of motion with different τ_c values, $T_{1\rho}$ is described by an equation that sums the term for each τ_c value (Eq. 3).

$$\frac{1}{T_{1\rho}} = \sum_{i=1}^{n} \frac{A_i\tau_{c,i}}{1+4\omega_1^2\tau_{c,i}^2} \tag{3}$$

The analysis of NMR relaxation times using an equation comprising multiple terms of τ_c has been reported for the T_1 of ^2H of $[Co(H_2O)_6][SiF_6]$ (42) and the T_1 and $T_{1\rho}$ of ^{19}F for flufenamic acid dispersed in PVP (Aso *et al.*, unpublished data). The same approach can be applied to the $T_{1\rho}$ of the lysozyme carbonyl carbons (Fig. 3) by assuming that the carbon has two different types of molecular motion with different τ_c values and that each τ_c shows an Arrhenius type of temperature dependence (Eq. 4).

$$\tau_c = \tau_0 \exp\left(\frac{E_a}{RT}\right) \tag{4}$$

The regression curve obtained for each molecular motion is shown in Fig. 8a, and the temperature dependence of τ_c for each motion is compared in Fig. 8b, which also includes the temperature dependence of α-relaxation time as calculated by the Vogel-Tammann-Fulcher (385 kJ/mol) and the Adam-Gibbs-Vogel equations (29) (123 kJ/mol) at temperatures above and below T_g, respectively. The T_g and the fragility parameter were assumed to be 130°C and 50 (16), respectively. The two types of motion observed for the

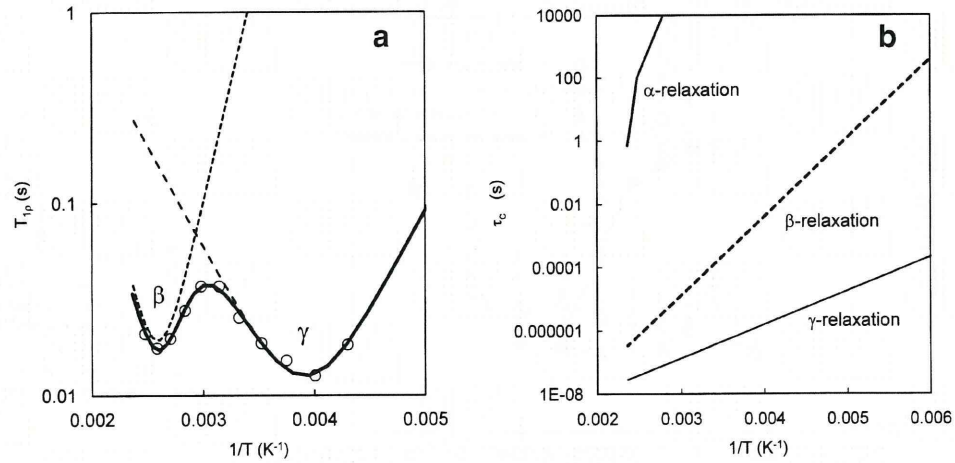

Fig. 8 (**a**) Regression curves for $T_{1\rho}$ of lysozyme carbonyl carbons in freeze-dried lysozyme obtained by assuming two different types of motion with different τ_c values. (**b**) Comparison of temperature coefficients of β- and γ-relaxation of lysozyme carbonyl carbons with that of α-relaxation time calculated assuming a T_g of 130°C and a fragility parameter of 50.

lysozyme carbonyl carbons revealed much smaller values of τ_c and Ea (i.e., slopes) than α-relaxation. The relaxation observed at higher temperatures showed a larger Ea and is referred to as β-relaxation in this paper. The other relaxation, observed at lower temperatures, is referred to as γ-relaxation. The parameters of $T_{1\rho}$(min), τ_0 and Ea were estimated to be 19 ms, 4×10^{-13} and 48 kJ/mol, respectively, for β-relaxation. For γ-relaxation, the parameters of $T_{1\rho}$ (min), τ_0 and Ea were estimated to be 13 ms, 9×10^{-11} and 20 kJ/mol, respectively.

The temperature dependence for the $T_{1\rho}$ of the lysozyme carbonyl carbons in the presence of sugars was also describable with a model that assumes that the carbon has two different types of molecular motion with different τ_c values, with each τ_c showing Arrhenius temperature dependence. The regression curves obtained for the freeze-dried lysozyme-trehalose, lysozyme-sucrose and lysozyme-isomaltose are shown in Fig. 9. The estimated parameters of $T_{1\rho}$(min) and Ea for β- and γ-relaxation are listed in Table I. The values of τ_c at 25°C calculated using these

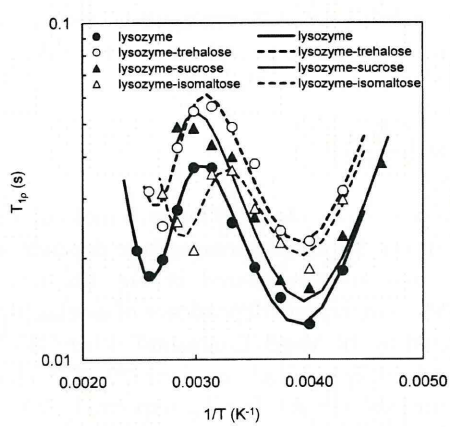

Fig. 9 Regression curves for $T_{1\rho}$ of lysozyme carbonyl carbons in lysozyme freeze-dried with sugars.

estimated parameters are also compared in Table I. The addition of sugars did not change the τ_c of the lysozyme carbonyl carbons or the Ea of τ_c for γ-relaxation. In contrast, τ_c for β-relaxation was increased by sucrose and decreased by isomaltose. Trehalose slightly decreased τ_c. The orders of τ_c and Ea for β-relaxation are as follows: sucrose > none > trehalose > isomaltose, although the standard errors in Ea make comparisons with pure lysozyme uncertain. These findings suggest that the mobility of the lysozyme carbonyl carbons is decreased by sucrose and increased by isomaltose. Because few data are available addressing the stability of freeze-dried lysozyme in the presence of sugars, the precise effect of sucrose on lysozyme stability is not known. However, the decrease in β-mobility brought about by sucrose may be related to the greater stabilizing effect of sucrose than trehalose, which was observed with some freeze-dried protein-sugar systems reported earlier (24,34).

The value of $T_{1\rho}$ minimum for the lysozyme carbonyl carbons shown in Table I varied with the sugars. The constant A in Eq. 1, which determines $T_{1\rho}$, is inversely proportional to the sixth power of the distance between the carbon and the proton that relaxes the carbon nuclei through dipole-dipole interaction (43). Thus, a small change in the distance between the carbon and proton nucleus results in a significant change in $T_{1\rho}$. The change in the estimated $T_{1\rho}$(min) caused by the addition of sugars suggests that the molecular structure of lysozyme is slightly changed by the sugars, such that the distance between the carbon and proton involved in nuclear relaxation is changed. The change in the value of $T_{1\rho}$ minimum caused by sucrose is smaller than that caused by trehalose and isomaltose, such that the change in the molecular structure of lysozyme caused by sucrose appears to be smaller than those caused by trehalose and isomaltose, which is curious in view of the fact that the apparent impact of sucrose on mobility (i.e., τ_c) is quite significant.

Table I Estimated Parameters of $T_{1\rho}$(min) and Ea for β- and γ-Relaxation, and Calculated τ_c Values at 25°C

Formulation	β -relaxation				γ-relaxation			
	τ_0 (s)	Ea (kJ/mol)	$T_{1\rho}$ (min) (ms)	τ_c (25°C) (ms)	τ_0 (s)	Ea (kJ/mol)	$T_{1\rho}$ (min) (ms)	τ_c (25°C) (μs)
lysozyme [a]	4×10^{-13} (2×10^{-12})	48 (14)	19 (4)	0.1	9×10^{-11} (2×10^{-10})	20 (4)	13 (3)	0.3
lysozyme-trehalose [b]	–	47 (1)	32 (7)	0.07	–	20 (0)	22 (2)	0.3
lysozyme-sucrose [c]	–	49 (1)	–	0.2	–	20 (0)	15 (2)	0.3
lysozyme-isomaltose [b]	–	43 (1)	28 (6)	0.02	–	20 (0)	20 (2)	0.3

() denotes standard error as provided by the non-linear regression

[a] Parameters of τ_0, Ea and $T_{1\rho}$(min) for each of the β- and γ-relaxation were evaluated by fit of the theoretical model (Eqs. 3 and 4) to the data.

[b] Parameters of Ea and $T_{1\rho}$(min) for each of the β- and γ-relaxation were estimated using the value of τ_0 obtained for lysozyme without sugars.

[c] The parameter Ea for β-relaxation was estimated using the values of τ_0 and $T_{1\rho}$(min) obtained for lysozyme without sugars, and parameters of Ea and $T_{1\rho}$(min) for γ-relaxation were estimated using the value of τ_0 obtained for lysozyme without sugars.

The value of apparent activation energy (i.e., temperature coefficient, Ea) determined for the β-relaxation of the lysozyme carbonyl carbons, shown in Table I, ranges between 43 to 50 kJ/mol, with the values for pure lysozyme and both the sucrose and trehalose systems being essentially the same but with the Ea for the isomaltose system being lower. By contrast, the Ea values for the γ-relaxation are all much smaller and essentially equal at around 20 kJ/mol. These Ea values are greater than those reported for fast dynamics of amorphous formulations determined by NMR relaxation measurements. For example, the apparent activation energy was determined to be 4.2 kJ/mol and 2.1 kJ/mol for the motion of the methine carbon in freeze-dried dextran and that of the protein carbonyl carbons in freeze-dried bovine serum γ-globulin, respectively, from NMR relaxation times (35). The dynamics of the PVP ring carbon and the sucrose methine carbon in freeze-dried PVP-sucrose mixtures, as determined by T_1 and $T_{1\rho}$, show apparent Ea values less than 10 kJ/mol. Moreover, the dynamics of the PVP ring carbon in freeze-dried PVP, determined by $T_{1\rho}$, exhibit a very small apparent Ea of 0.8 kJ/mol (36). These small apparent activation energies evaluated from the temperature dependence of NMR relaxation times, which are too small to be interpreted in terms of an activated state kinetic model, may be attributed to the invalid assumption that the atom of interest has only a single type of motion with a single τ_c value. When the atom has multiple types of motion with different τ_c values, the Ea value determined in a temperature range near $T_{1\rho}$ maximum according to this analysis has no sound theoretical foundation and may have no physical meaning as an activation energy. The analysis of NMR relaxation time according to a multiple-dynamic model, as described in this paper, is necessary to determine Ea for the individual type of motion. The value of Ea observed for freeze-dried lysozyme-sugar systems in this study is much smaller than the Ea for alpha relaxation for freeze-dried trehalose (145 kJ/mol) and freeze-dried sucrose (225 kJ/mol) as determined by isothermal microcalorimetry (28), calculated using β=0.4, but comparable to those for freeze-dried lactose by dielectric relaxation spectroscopy (72 kJ/mol and 52 kJ/mol for β- and γ-relaxation, respectively) (32).

The value of Ea determined for molecular motions in freeze-dried formulations is one of the basic clues for exploring the molecular motion most relevant to the instability of freeze-dried formulations. For example, if a certain motion shows an Ea value that is markedly different from the activation energy for degradation, it seems likely[1] that this motion may be excluded from the candidate motions responsible for the instability. The values of Ea determined for the β-relaxation of the lysozyme carbonyl carbons in this study are comparable to the values of activation energy for degradation observed for freeze-dried formulations as described below, suggesting correlations between β-relaxation and instability. Few data on activation energy have been reported for degradation in freeze-dried formulations, but Ea can be calculated from the Arrhenius plots of the apparent rate constants reported for degradation in freeze-dried formulations. For example, the Ea of the hydrolysis rate of cephalothin freeze-dried with dextran was calculated to be about 50 kJ/mol; Ea of 46 kJ/mol was calculated for acetyl transfer reaction between aspirin and sulfadiazine freeze-dried with poly(vinylpyrrolidone) (14). For degradation of freeze-dried proteins, 63 kJ/mol for aggregation of β-galactosidase freeze-dried with sugars (24), 50 kJ/mol for β-galactosidase freeze-dried with polyvinylalcohol (12), 67 kJ/mol for degradation of insulin freeze-dried with PVP (18).

[1] This statement is equivalent to stating that the motion represented by the relaxation process may have nothing directly to do with the motion required for degradation, if the "coupling coefficient" relating a relaxation time constant for a given microstate with degradation within that microstate, which has been discussed in a reference (6), is much less than unity.

Effect of Sub-T_g Heating on the Mobility of Lysozyme Carbonyl Carbons

Annealing of freeze-dried formulations at temperatures below and near the T_g is well known to increase α-relaxation time and to stabilize the formulations (41). For the freeze-dried lysozyme-trehalose and lysozyme-sucrose, the $T_{1\rho}$ value obtained immediately after the temperature was raised from −40°C to 62°C was close to the value determined at 62.3°C without heating or cooling (Fig. 3), as shown in Fig. 4. Thereafter, $T_{1\rho}$ decreased with time and became roughly constant within several hours. This finding suggests that the β- and γ-relaxations of lysozyme at the time point immediately after the temperature increase is different from those of lysozyme heated at 62°C for several hours.

As shown in Fig. 5, the $T_{1\rho}$ of the protein carbonyl carbons observed at temperatures below 0°C was not significantly affected by heating at 62°C for 8 h, but $T_{1\rho}$ above 0°C was greatly decreased by heating. The V-shaped temperature dependence of $T_{1\rho}$ for γ-relaxation was widened and moved toward a higher temperature range both for trehalose and sucrose. These findings suggest that the average τ_c for all carbonyl carbons in the lysozyme molecule is increased after heating and also that carbonyl carbons at different sites of the lysozyme molecule are affected by the heating treatment in varying degrees from each other, such that the range of τ_c for γ-relaxation of the lysozyme carbonyl carbons is widened. The effect of heating on the β-relaxation is not clear because of more limited $T_{1\rho}$ data. However, the finding that the $T_{1\rho}$ minimum for β-relaxation of the freeze-dried lysozyme-trehalose observed before heating is not observed after heating in the temperature range studied suggests that the $T_{1\rho}$ minimum for β-relaxation is shifted to a higher temperature by heating. Thus, both β- and γ-relaxations appear to be slowed by heating in a manner similar to the annealing effects on α-relaxations.

Mobility of Sugars Freeze-Dried with Lysozyme

The temperature dependence for the $T_{1\rho}$ of trehalose, sucrose and isomaltose carbons (Figs. 5 and 6) exhibits $T_{1\rho}$ minima in a similar temperature range as for the $T_{1\rho}$ of the lysozyme carbonyl carbons. This suggests that the sugar carbons have motions with similar τ_c values as the β- and γ-relaxation of the protein carbonyl carbons. Here, the values of $T_{1\rho}$ for the sucrose carbon are greater than those for the trehalose and isomaltose methine carbon. This is expected because the sucrose carbon (C-1) has no proton directly binding to the carbon, while trehalose and isomaltose methine carbons have a proton directly binding to the carbon. The rate of spin-lattice relaxation depends on the number of the protons that cause dipole-dipole interaction with the carbon, leading to spin-lattice relaxation, as well as the distance between the proton and the carbon (C-1). More protons and a shorter distance both lead to faster spin-lattice relaxation. The spin-lattice relaxation of sucrose carbon (C-1) is slower than that of trehalose and isomaltose, because the proton involved in the dipole-dipole interaction with the carbon (C-1) in the sucrose system is at a greater distance from the carbon compared to the trehalose and isomaltose systems.

The temperature dependence for the $T_{1\rho}$ of sugar carbons was not significantly changed by the addition of lysozyme. This finding means that the motions of sugar carbons with similar τ_c values as the β- and γ-relaxation of the protein carbonyl carbons are not affected by interaction with lysozyme. This finding is in contrast to the observation that the β- and γ-relaxations of the lysozyme carbonyl carbons are affected by interaction with the sugars (Table I). This difference may be explained by assuming that the sugar induces conformational changes in the protein, such that the mobility of the protein carbonyl carbons is significantly changed but mobility of the sugar carbon is changed by interaction with the protein only for the carbons involved in the interaction. Mobility of the carbons that are not involved in the interaction also contributes to the determined $T_{1\rho}$ value, such that the measured $T_{1\rho}$ for the sugar is not sensitive to the interaction with protein.

The $T_{1\rho}$ of the methyl carbon of ^{13}C-methylated isomaltose decreases rapidly as temperature increases near and above T_g (Fig. 7). This finding suggests that the motion of the methyl carbon, which is speculated to be much faster than the carbon (C-1), is coupled with structural relaxation since structural relaxation shows strong temperature dependence near T_g. This observation is in contrast to the general concept that the fast motion of side chains is generally independent of structural relaxation.

CONCLUSION

The temperature dependence for the $T_{1\rho}$ of the lysozyme carbonyl carbons in freeze-dried lysozyme with and without sugars (trehalose, sucrose and isomaltose) was describable with a model that assumes that the carbon has two different types of molecular motion with different τ_c values and that each τ_c shows an Arrhenius type of temperature dependence. A single relaxation mode is not consistent with the data, meaning that interpretation of relaxation time data is complex and may demand data over an extended temperature range. If $T_{1\rho}$ is determined in a temperature range near $T_{1\rho}$ maximum, simply observing that an increase in temperature reduces $T_{1\rho}$ does not necessarily mean that the

$T_{1\rho}$ measured is directly proportional to the correlation time, τ_c, nor is the temperature coefficient of $T_{1\rho}$ necessarily a good measure of the activation energy of a single process. Further, trends in $T_{1\rho}$ with formulation determined in this temperature range may not necessarily be predictive of trends in molecular mobility.

Lysozyme carbonyl carbons in the absence of sugars revealed two types of motion with much smaller values of τ_c and Ea than structural relaxation: a motion with a τ_c of 1×10^{-4} s at 25°C and an Ea of 48 kJ/mol (β-relaxation), and another faster motion with a τ_c of 3×10^{-7} s at 25°C and an Ea of 20 kJ/mol (γ-relaxation). Addition of sugars does impact the mobility of lysozyme, as evidenced by the impact of sugars on the values of τ_c and Ea. The τ_c and Ea for β-relaxation were increased by the addition of sucrose and decreased by the addition of trehalose and isomaltose. The orders of τ_c and Ea are as follows: sucrose > none > trehalose > isomaltose, suggesting that the β-mobility of the lysozyme carbonyl carbons is significantly decreased by sucrose but increased by isomaltose.

REFERENCES

1. Yoshioka S, Aso Y. Correlation between molecular mobility and chemical stability during storage of amorphous pharmaceuticals. J Pharm Sci. 2007;96:960–81.
2. Craig DQM, Royall PG, Kett VL, Hopton ML. The relevance of the amorphous state to pharmaceutical dosage forms: glassy drugs and freeze dried systems. Int J Pharm. 1999;179:179–207.
3. Wang W. Lyophilization and development of solid protein pharmaceuticals. Int J Pharm. 2000;203:1–60.
4. Parker R, Gunning YM, Lalloué B, Noel TR, Ring SG. Glassy state dynamics, its significance for biostabilization and role of carbohydrates. In: Levine H, editor. Amorphous food and pharmaceutical systems. Cambridge: The Royal Society of Chemistry; 2002. p. 73–87.
5. Pikal MJ. Chemistry in solid amorphous matrices: implication for biostabilization. In: Levine H, editor. Amorphous food and pharmaceutical systems. Cambridge: The Royal Society of Chemistry; 2002. p. 257–72.
6. Pikal MJ. Mechanisms of protein stabilization during freeze-drying and storage: the relative importance of thermodynamic stabilization and glassy state relaxation dynamics. In: Rey L, May JC, editors. Freeze-drying/lyophilization of pharmaceutical and biological products. 2nd ed. New York: Marcel Dekker Inc; 2004. p. 63–107.
7. Shamblin SL. The role of water in physical transformations in freeze-dried products. In: Costantino HR, Pikal MJ, editors. Lyophilization of biopharmaceuticals. Arlington: AAPS; 2004. p. 229–70.
8. Lechuga-Ballesteros D, Miller DP, Dudddu SP. Thermal analysis of lyophilized pharmaceutical peptide and protein formulations. In: Costantino HR, Pikal MJ, editors. Lyophilization of biopharmaceuticals. Arlington: AAPS; 2004. p. 271–335.
9. Stots CE, Winslow SL, Houchin ML, D'Souza AJM, Ji J, Topp EM. Degradation pathways for lyophilized peptides and proteins. In: Costantino HR, Pikal MJ, editors. Lyophilization of biopharmaceuticals. Arlington: AAPS; 2004. p. 443–79.
10. Sun WQ, Davidson P, Chan HSO. Protein stability in the amorphous carbohydrate matrix: relevance to anhydrobiosis. Biochim Biophys Acta. 1998;1425:245–54.
11. Yoshioka S, Aso Y, Nakai Y, Kojima S. Effect of high molecular mobility of poly(vinyl alcohol) on protein stability of lyophilized γ-globulin formulations. J Pharm Sci. 1998;87:147–51.
12. Yoshioka S, Tajima S, Aso Y, Kojima S. Inactivation and aggregation of β-galactosidase in lyophilized formulation described by Kohlrausch-Williams-Watts stretched exponential function. Pharm Res. 2003;20:1655–60.
13. Lai MC, Hageman MJ, Schowen RL, Borchardt RT, Laird BB, Topp EM. Chemical stability of peptide in polymers. 2. Discriminating between solvent and plasticizing effects of water on peptide deamidation in poly(vinylpyrrolidone). J Pharm Sci. 1999;88:1081–9.
14. Yoshioka S, Aso Y, Kojima S. Temperature- and glass transition temperature-dependence of bimolecular reaction rates in lyophilized formulations described by the Adam-Gibbs-Vogel equation. J Pharm Sci. 2004;93:1062–9.
15. Guo Y, Byrn SR, Zografi G. Physical characteristics and chemical degradation of amorphous quinapril hydrochloride. J Pharm Sci. 2000;89:128–43.
16. Yoshioka S, Aso Y. A quantitative assessment of the significance of molecular mobility as a determinant for the stability of lyophilized insulin formulations. Pharm Res. 2005;22:1358–64.
17. Yoshioka S, Miyazaki T, Aso Y. Degradation rate of lyophilized insulin, exhibiting an apparent arrhenius behavior around glass transition temperature regardless of significant contribution of molecular mobility. J Pharm Sci. 2006;95:2684.
18. Yoshioka S, Aso Y, Miyazaki T. Negligible contribution of molecular mobility to the degradation rate of insulin lyophilized with poly(vinylpyrrolidone). J Pharm Sci. 2006;95:939–43.
19. Strickley RG, Anderson BD. Solid-state stability of human insulin II. Effect of water on reactive intermediate partitioning in lyophiles from pH 2–5 solutions: stabilization against covalent dimer formation. J Pharm Sci. 1997;86:645–53.
20. Yoshioka S, Miyazaki T, Aso Y. β-relaxation of insulin molecule in lyophilized formulations containing trehalose or dextran as a determinant of chemical reactivity. Pharm Res. 2006;23:961–6.
21. Chang L, Shepherd D, Sun J, Ouellete D, Grant KL, Tang X, *et al.* Mechanism of protein stabilization by sugar during freeze-drying and storage: native structure preservation, specific interaction, and/or immobilization in a glassy matrix? J Pharm Sci. 2005;94:1427–44.
22. Cicerone MS, Soles C. Fast dynamics and stabilization of proteins: binary glasses of trehalose and glycerol. Biophys J. 2004;86:3836–45.
23. Cicerone MT, Soles CL, Chowdhuri Z, Pikal MJ, Chang LL. Fast dynamics as a diagnostic for excipients in preservation of dried proteins. Am Pharm Rev. 2005;8:24–7.
24. Yoshioka S, Miyazaki T, Aso Y, Kawanishi T. Significance of local mobility in aggregation of β-galactosidase lyophilized with trehalose, sucrose or stachyose. Pharm Res. 2007;24:1660–7.
25. Matsuo M, Bin Y, Xu C, Ma L, Nakaoki T, Suzuki T. Relaxation mechanism in several kinds of polyethylene estimated by dynamic mechanical measurements, positron annihilation, X-ray and ^{13}C solid-state NMR. Polymer. 2003;44:4325–40.
26. Aso Y, Yoshioka S. Effect of freezing rate on physical stability of lyophilized cationic liposomes. Chem Pharm Bull. 2005;53:301–4.
27. Andronis V, Zografi G. Molecular mobility of supercooled amorphous indomethacin, determined by dynamic mechanical analysis. Pharm Res. 1991;14:410–4.
28. Liu J, Rigsbee DR, Stotz C, Pikal MJ. Dynamics of pharmaceutical amorphous solids: the study of enthalpy relaxation by isothermal microcalorimetry. J Pharm Sci. 2002;91:1853–62.

29. Shamblin SL, Tang X, Chang L, Hancock BC, Pikal MJ. Characterization of the time scales of molecular motion in pharmaceutically important glasses. J Phys Chem B. 1999;103:4113–21.
30. Kumagai H, Sugiyama T, Iwamoto S. Effect of water content on dielectric relaxation of gelatin in a glassy state. J Agric Food Chem. 2000;48:2260–5.
31. Yoshioka S, Aso Y. Glass transition- related changes in molecular mobility below glass transition temperature of freeze-dried formulations, as measured by dielectric spectroscopy and solid state nuclear magnetic resonance. J Pharm Sci. 2005;94:275–87.
32. Ermolina I, Polygalov E, Bland C, Smith G. Dielectric spectroscopy of low-loss sugar lyophiles: II. Relaxation mechanisms in freeze-dried lactose and lactose monohydrate. J Non-Crystalline Solids. 2007;353:4485–91.
33. Correia NT, Ramos JJM, Descamps M, Collins G. Molecular mobility and fragility inindomethacin: a thermally stimulated depolarization current study. Pharm Res. 2001;18:1767–74.
34. Pikal MJ, Rigsbee D, Roy ML, Galreath D, Kovach KJ, Wang B, *et al.* Solid state chemistry of proteins: II. the correlation of storage stability of freeze-dried human growth hormone (hGH) with structure and dynamics in the glassy solid. J Pharm Sci. 2008;97:5106–21.
35. Yoshioka S, Aso Y, Kojima S, Sakurai S, Fujiwara T, Akutsu H. Molecular mobility of protein in lyophilized formulations linked to the molecular mobility of polymer excipients, as determined by high resolution ^{13}C solid-state NMR. Pharm Res. 1999;16:1621–5.
36. Aso Y, Yoshioka S, Zhang J, Zografi G. Effect of water on the molecularmobility of sucrose and poly(vinylpyrrolidone) in a colyophilized formulation as measured by ^{13}C-NMR relaxation time. Chem Pharm Bull. 2002;50:822–6.
37. Latosinska JN, Latosinska M, Utrecht R, Mielcarek S, Pietrzak J. Molecular dynamics of solid benzothiadiazine derivatives (Thiazides). J Molecular Structure. 2004;694:211–7.
38. Niehaus Jr WG, Ryhage R. Determination of double bond positions in polyunsaturated fatty acids by combination gas chromatography-mass spectrometry. Anal Chem. 1968;40:1840–7.
39. Bielecki A, Burum DP. Temperature dependence of ^{207}Pb MAS spectra of solid lead nitrate. An accurate, sensitive thermometer for variable-temperature MAS. K Magnetic Res Ser A. 1995;116:215–20.
40. Pfeffer PE, Odier L, Dudley RL. Assignment of ^{13}C CPMAS NMR spectra of crystalline methyl β-D-glucopyranoside and sucrose using deuterium labeling and interrupted proton decoupling. J Carbohydrate Chem. 1990;9:619–29.
41. Wang B, Cicerone MT, Aso Y, Pikal MJ. The impact of thermal treatment on the stability of freeze-dried amorphous pharmaceuticals: II. Aggregation in an IgG1 fusion protein. J Pharm Sci. 2010;99:683–700.
42. Iijima T, Mizuno M, Suhara M, Endo K. Molecular and electron-spin dynamics in $[M(H_2O)_6][AB_6]$ as studied by solid state NMR. Bunseki Kagaku. 2003;52:157–63.
43. Horii F. NMR relaxation and dynamics. In: Ando I, Asakura T, editors. Solid state NMR of polymers. Amsterdam: Elsevier; 1998. p. 51–81.

RESEARCH ARTICLE

Feasibility of Atomic Force Microscopy for Determining Crystal Growth Rates of Nifedipine at the Surface of Amorphous Solids with and Without Polymers

TAMAKI MIYAZAKI, YUKIO ASO, TORU KAWANISHI

Division of Drugs, National Institute of Health Sciences, Setagaya-ku, Tokyo 158-8501, Japan

Received 21 February 2011; revised 31 March 2011; accepted 18 April 2011

Published online in Wiley Online Library (wileyonlinelibrary.com). DOI 10.1002/jps.22603

ABSTRACT: Amorphous nifedipine (NFD), which has a smooth surface immediately after preparation, was shown to have structures resembling clusters of curling and branching fibers approximately 1 μm wide by atomic force microscopy (AFM) after storage at 25°C. The size of the cluster-like structures increased with storage over time, implying crystal growth. The average elongation rate of the fibers determined by AFM at ambient room temperature was 1.1×10^{-9} m/s, and this agreed well with the crystal growth rate of 1.6×10^{-9} m/s determined by polarized light microscopy. The crystal growth rate of NFD in solid dispersions with 5% polyethylene glycol (PEG) was found to be 5.0×10^{-8} m/s by AFM. Although this value was approximately the same as that obtained by polarized light microscopy, three-dimensional information obtained by AFM for the crystallization of NFD in a solid dispersion with PEG revealed that the changes in topography were not a consequence of surface crystal growth, but rather attributable to the growth of crystals formed in the amorphous bulk. For solid dispersions with α,β-poly(N-5-hydroxypentyl)-L-aspartamide, acceleration of NFD crystallization by tapping with an AFM probe was observed. The present study has demonstrated the feasibility and application of AFM for interpretation of surface crystallization data. © 2011 Wiley-Liss, Inc. and the American Pharmacists Association J Pharm Sci

Keywords: amorphous; crystallization; excipients; physical stability; solid dispersion; microscopy

INTRODUCTION

Amorphous drugs are generally more soluble and dissolve faster than their crystalline counterparts.[1–3] Therefore, amorphization of poorly water-soluble drugs is a useful method for enhancing their dissolution rate and consequently improving their bioavailability. However, the amorphous form is thermodynamically unstable and tends to revert to its crystalline form, resulting in loss of the solubility advantage. Recently, surface-enhanced crystallization of indomethacin[4] and nifedipine (NFD)[5] has been reported. The crystal growth rates of amorphous indomethacin and NFD at the free surface were orders of magnitude faster than those in bulk at temperatures below their glass transition temperature (T_g). Microscopic observation of partially crystallized indomethacin and NFD samples has revealed that crystallized drugs are localized at the surface of the samples.[5] Once the surface is covered with a crystal layer, the solubility advantage is lost even if the most interior part of the solid remains amorphous.

Atomic force microscopy (AFM), which can capture surface topography images of solid samples with a resolution of the micrometer order or less, may be a useful tool for investigating the surface crystallization of pharmaceuticals. The crystallization of cholesterol under conditions simulating the gallbladder environment has been studied by AFM.[6] Cholesterol crystals of submicrometer size have been observed on the surface of mica and mucin-coated mica, but no such crystals have been found on the surface of silanized mica, suggesting that a network of hydrogen bonds on the surface provides favorable conditions for the nucleation and growth of cholesterol crystals. Molecular rearrangements at the surface have been observed for caffeine/carboxylic acid cocrystals by AFM.[7] The depth and width of trenches aligned

Correspondence to: Tamaki Miyazaki (Telephone: +81-3-3700-1141; Fax: +81-3-3707-6950; E-mail: miyazaki@nihs.go.jp)

Journal of Pharmaceutical Sciences